ABOUT STAGS, a general-purpose finite element shell analysis computer program by Dr. Charles C. Rankin, Bo. O. Almroth, and others.

The following text is included in the paper, "Optimization of an axially compressed ring and stringer stiffened cylindrical shell with a general buckling modal imperfection", AIAA 48th Structures, Structural Dynamics, and Materials Conference, Paper no. AIAA-2007-2216, 2007. Tables and figures referred to here are in that paper.

Section 4.0 of the paper cited above was written by Dr. Charles C. Rankin
(email address: **crankin@rhombuscgi.com**), one of the developers of the STAGS computer program.

4.0 DESCRIPTION OF STAGS [18-21]

In most of the PANDA2 references listed under [1] and in [22, 23] and in this paper optimum designs obtained by PANDA2 are evaluated later via STAGS models.

STAGS (**ST**ructural **A**nalysis of **G**eneral **S**hells [18–21]) is a finite element code for **general-purpose nonlinear analysis of stiffened shell structures of arbitrary shape** and complexity. Its capabilities include stress, stability, vibration, and transient analyses with both material and geometric nonlinearities permitted in all analysis types. STAGS includes enhancements, such as a higher order thick shell element, more advanced nonlinear solution strategies, and more comprehensive post-processing features such as a link with STAPL, a postprocessor used to generate many of the figures in this paper: figures that display the STAGS model, such as Figs. 1a-c and 2, for example.

Research and development of STAGS by Rankin, Brogan, Almroth, Stanley, Cabiness, Stehlin and others, formerly of the Computational Mechanics Department of the Lockheed Martin Advanced Technology Center, has been under continuous sponsorship from U.S. government agencies for the past 40 years. During this time particular emphasis has been placed on improvement of the capability to solve difficult nonlinear problems such as the prediction of the behavior of axially compressed stiffened panels loaded far into their locally post-buckled states. STAGS has been extensively used worldwide for the evaluation of stiffened panels and shells loaded well into their locally post-buckled states. See [21], for example.

A large rotation algorithm that is independent of the finite element library has been incorporated into STAGS [20B]. With this algorithm there is no artificial stiffening due to large rotations. The finite elements in the STAGS library do not store energy under arbitrary rigid-body motion, and the first and second variations of the strain energy are consistent. These properties lead to quadratic convergence during Newton iterations.

Solution control in nonlinear problems includes specification of load levels or use of the **advanced Riks-Crisfield path parameter [21]** that enables traversal of limit points into the post-buckling regime. Two load systems with different histories (Load Sets A and B) can be defined and controlled separately during the solution process. Flexible restart procedures permit switching from one strategy to another during an analysis, including shifts from bifurcation buckling to nonlinear collapse analyses and back and shifts from static to transient and transient to static analyses with modified boundary conditions and loading. STAGS provides

solutions to the generalized eigenvalue problem for **buckling** and vibration **from a linear (Fig. 24) or nonlinear (Figs. 26, 27) stress state.**

Quadric surfaces can be modeled with minimal user input as individual substructures called **"shell units"** in which the analytic geometry is represented exactly. "Shell units" can be connected along edges or internal grid lines with partial or complete compatibility. In this way complex structures can be assembled from relatively simple units. Alternatively, a structure of arbitrary shape can be modeled with use of an "element unit".

Geometric imperfections can be generated automatically in a variety of ways, thereby permitting imperfection-sensitivity studies to be performed. For example, **imperfections can be generated by superposition of several buckling modes determined from previous linear and nonlinear STAGS analyses of a given case**. (See Parts 4-7 of Table 9 and Figs. 24, 26, and 27, for example).

A variety of material models is available, including both plasticity and creep. STAGS handles isotropic and anisotropic materials, including composites consisting of up to 60 layers of arbitrary orientation. Four plasticity models are available, including isotropic strain hardening, the White Besseling (mechanical sub-layer model), kinematic strain hardening, and deformation theory.

Two independent load sets, each composed from simple parts that may be specified with minimal input, define a spatial variation of loading. Any number of point loads, prescribed displacements, line loads, surface tractions, thermal loads, and "live" pressure (hydrostatic pressure which remains normal to the shell surface throughout large deformations) can be combined to make a load set. For transient analysis the user may select from a menu of loading histories, or a general temporal variation may be specified in a user-written subroutine.

Boundary conditions (B.C.) may be imposed either by reference to certain standard conditions or by the use of single- and multi-point constraints. Simple support, symmetry, anti-symmetry, clamped, or user-specified B.C. can be defined on a "shell unit" edge. Single-point constraints that allow individual freedoms to be free, fixed, or a prescribed non-zero value may be applied to grid lines and surfaces in "shell units" or "element units". A useful feature for buckling analysis allows these constraints to differ for the pre-buckling stress and eigenvalue analyses. Langrangian constraint equations containing up to 100 terms may be defined to impose multi-point constraints.

STAGS has a variety of finite elements suitable for the analysis of stiffened plates and shells. Simple four node quadrilateral plate elements with a cubic lateral displacement field (called "410" and "411" elements) are effective and efficient for the prediction of post-buckling thin shell response. A linear (410) or quadratic (411) membrane interpolation can be selected. For thicker shells in which transverse shear deformation is important **(and for the thin-shell cases described in this paper),** STAGS provides the **Assumed Natural Strain (ANS) nine node element (called "480" element).** A two node beam element compatible with the four node quadrilateral plate element is provided to simulate stiffeners and beam assemblies. Other finite elements included in STAGS are described in the STAGS literature [18-21].

5.0 WHY MUST STAGS OR SOME OTHER GENERAL-PURPOSE CODE BE USED TO CHECK OPTIMUM DESIGNS FROM PANDA2?

PANDA2 uses many approximations and "tricks" in models for stress and buckling. Some of these are

described in Sections 8 - 10 of [1K]. For example, knockdown factors are derived to compensate for the inherent unconservativeness of smearing stiffeners [1K] and to account for the effects of transverse shear deformation [1A]. The effect of initial local, inter-ring, and general imperfections in the shapes of critical local, inter-ring, and general buckling modes are accounted for in an approximate manner as described in [1D] and [1E]. The distribution of pre-buckling stress resultants in the various segments of a discretized skin-stringer module [1A and Fig. 4 in this paper] and of a "skin"-ring discretized module [1G] of an imperfect and therefore initially bent stiffened shell are approximate. For example, stabilizing (**tensile**) axial and hoop resultants in the panel skin that arise from pre-buckling bending of an initially globally imperfect shell are neglected in order to avoid the production of unconservative optimum designs.

PANDA2 has been developed over the years with the philosophy that the use of many relatively simple approximate models will lead to optimum designs that are reasonable and for which no complicated "combined" modes of failure will inadvertently be missed. Because of the approximate nature of these multiple simple PANDA2 models, one **MUST** use STAGS or some other general-purpose finite element code to evaluate optimum designs obtained by PANDA2.

The particular advantage of using STAGS is that there exists a PANDA2 processor called STAGSUNIT [1**I**] that automatically generates input files, ***.bin** and ***.inp**, for STAGS. As described in [1**I**], the processor STAGSUNIT is written in such a way that "patches" (sub-domains) of various portions of a complete panel or shell can be analyzed with STAGS. **The correct pre-buckled state of a perfect panel is preserved independently of the size of the "patch" to be included in the STAGS sub-domain model**. The minimum size "patch" must contain at least one stiffener spacing in each coordinate direction. In a stringer-stiffened shell stringers are always included along the two straight edges of the "patch". There may or may not be rings running along the two curved edges of the "patch", depending on input to STAGSUNIT provided by the user of PANDA2. **Stiffeners that run along the four boundaries of the "patch" have half the stiffness and half the loading of those that lie within the "patch".** It is primarily this characteristic of the STAGS models produced by STAGSUNIT that preserves the correct pre-buckled state of the "patch" independently of its size.

The STAGS models are constructed by the PANDA2 processor, STAGSUNIT, in such a way that all stiffeners are connected only to the panel skin. That is, where stiffeners intersect they simply pass through one another with no constraints between them along their lines of intersection, if any. This is a conservative model with respect to buckling. The same model is used in PANDA2. The STAGSUNIT processor can generate models in which all stiffeners may be composed of shell units, one or more sets of stiffeners may be composed of beams, or one or more sets of stiffeners may be "smeared" as prescribed by Baruch and Singer [12].

6.0 HOW TO USE STAGS FOR THE ANALYSIS OF IMPERFECT STIFFENED CYLINDRICAL SHELLS

In order to use STAGS to evaluate a shell with a general buckling modal imperfection, one must:

1. Obtain an optimum design with PANDA2 via multiple executions of SUPEROPT [1D, 1K, and Fig. 3 and Table 3 in this paper].

2. Use STAGSUNIT [1**I**] to generate input files, ***.bin** and ***.inp**, for STAGS operating in its linear bifurcation buckling mode (STAGS analysis type index INDIC=1). Generate various *.inp files corresponding to various models, as described next.

3. Explore at least two **preliminary linear buckling** models with the STAGS input index ILIN=0 [20**C**] in each shell unit (Runs 1 and 2 in Part 1 of Table 9). In each model ask for about 8 eigenvalues (*.bin file) so that in the case of closely spaced eigenvalues a general buckling mode shape similar to that determined by PANDA2 will be found. The purpose of these preliminary runs is to obtain good and better estimates of the critical **general** buckling mode shape and load factor (eigenvalue). The most accurate general buckling load factor is to be used as the initial **"eigenvalue shift"** (see Parts 2 and 3 of Table 9 and [20C]) in the *.bin file for models of the type described in the next item (Item 4). Two preliminary models are:

a. 1st linear buckling model: **all stiffeners smeared** (Figs. 37 and 38, for example)
b. 2nd linear buckling model: **stringers smeared, rings as shell units** (2 shell units per ring for a T-shaped ring, one for the ring web and the other for the outstanding flange of the ring) (Figs. 39 and 40, for example).

4. Decide how much of the shell circumference to include in the most refined STAGS model. The circumferential domain should permit one **full** circumferential wave of the critical general buckling mode determined in Model 3b (previous item), that is, the general buckling mode that most resembles that predicted by PANDA2. Symmetry conditions should be applied to the two opposite straight edges (generators) of the model of the cylindrical shell (Runs 3 and Runs 5-7 in Part 1 of Table 9 and Fig. 21a, for example).

5. Decide how to concentrate nodal points in Model 4 in order accurately to capture all possible buckling modes (local stiffener buckling, local skin buckling, inter-ring buckling, stiffener rolling, and general buckling) (Run 8 in Part 1 of Table 9). One can refer to the margins listed in the PANDA2 output file, *.OPM, corresponding to the optimized design in order to establish reasonable nodal point densities to guarantee converged behavior because the phrases that define these margins contain the critical numbers of axial and circumferential half-waves in the various buckling modes. (See the top part of Table 7 and Figs. 26 and 27, for example).

6. With the use of Model 5, run STAGS multiple times in its **linear bifurcation buckling** branch (INDIC=1) with various **"eigenvalue shifts"** in order to find one or more **general buckling modes**. (See Part 2 of Table 9). One or more of these modes are to be used as imperfection shapes in future nonlinear static and dynamic STAGS runs. The initial "eigenvalue shift" should be close to (perhaps slightly under) that predicted from Model 3b. If the critical general buckling mode is "polluted" by a short-wavelength component, such as that shown in Figs. 23 and 24 of [1**I**] and in Fig. 75 in this paper, try running again with the STAGS index ILIN = 1 [20**C**] in every shell unit instead of ILIN= 0. ILIN=1 "filters out" many short-wavelength buckling modes, thus making it easier to find the few general buckling modes "hidden" in the dense eigenvalue spectrum and less likely that a "dirty" general buckling mode such as that displayed in Fig. 75 will occur. See, for example, Fig. 76. If changing ILIN from 0 to 1 does not solve this problem, one can make seemingly insignificant alterations in the nodal point distribution and run again. Experience with numerous STAGS models seems to indicate that "dirty" general buckling modes such as that displayed in Fig. 75 arise when a mode corresponding to short-wavelength buckling is associated with an eigenvalue that is extremely close (the same to five significant figures, for example) to that corresponding to the critical general buckling mode. "Jiggling" the finite element model causes the eigenvalues to shift slightly, those corresponding to a general buckling mode shifting less than those corresponding to short-wavelength buckling modes. **It is important to obtain a "clean" general buckling mode** because short-wavelength components in the initial imperfection shape, such as that displayed if Fig. 75, give rise to significant local bending stresses obtained from future nonlinear STAGS runs, bending stresses of a nature that are extremely unlikely to occur in an actual fabricated shell.

7. Edit the *.bin and *.inp files (or run STAGSUNIT again with different input) to prepare for a **nonlinear static equilibrium** run with STAGS (STAGS analysis type index INDIC=3). Include at least one general buckling modal imperfection in the *.inp file, such as that shown in Fig. 24. (See Part 5 of Table 9 and Fig. 25). Choose carefully **both** the **amplitude** of the general buckling modal imperfection and its **sign**.

8. Run the nonlinear static (INDIC=3) STAGS case and inspect the results after execution. (See Part 6 in Table 9).

9. Multiple nonlinear static STAGS runs are usually required to obtain a **collapse** load. With each run it may be necessary to **add one or more nonlinear bifurcation buckling modes**, such as those shown in Figs. 26 and 27, as additional imperfection shapes in order to "trigger" collapse or to avoid nonlinear bifurcation points that lie on or near the nonlinear equilibrium path [1H, 22]. (See Sub-section 18.5 of [1K] and Parts 6 – 9 of Table 9 and Figs. 26-29 in this paper).

10. It may be necessary to follow Step 9 with a series of **nonlinear dynamic** STAGS runs [23] in order to determine the maximum load-bearing capability of a shell. This step is used in the STAGS analysis of the "testax3" case in [1K], as described in Section 18.0 of [1K]. This step is used for most of the cases explored in this paper. (See Parts 10 – 13 of Table 9 and Figs. 30-32).

19.0 REFERENCES

[1] Bushnell, D., et al, (**A**) "PANDA2 - Program for minimum weight design of stiffened, composite, locally buckled panels", Computers and Structures, Vol. 25 (1987) pp. 469-605. See also: (**B**) "Theoretical basis of the PANDA computer program for preliminary design of stiffened panels under combined in-plane loads", Computers and Structures, v. 27, No. 4, pp 541-563, 1987; (**C**) "Optimization of composite, stiffened, imperfect panels under combined loads for service in the postbuckling regime", Computer Methods in Applied Mechanics and Engineering, Vol. 103, pp 43-114, 1993; (**D**) "Recent enhancements to PANDA2" 37th AIAA Structures, Dynamics, and Materials (SDM) Conference, April 1996; (**E**) "Approximate method for the optimum design of ring and stringer stiffened cylindrical panels and shells with local, inter-ring, and general buckling modal imperfections", Computers and Structures, Vol. 59, No. 3, 489-527, 1996, with W. D. Bushnell; (**F**) "Optimum design via PANDA2 of composite sandwich panels with honeycomb or foam cores", AIAA Paper 97-1142, AIAA 38th SDM Conference, April 1997; (**G**) "Additional buckling solutions in PANDA2", AIAA 40th SDM Conference, p 302-345, April 1999, with H. Jiang and N. F. Knight, Jr.; (**H**) "Minimum-weight design of a stiffened panel via PANDA2 and evaluation of the optimized panel via STAGS", Computers and Structures, Vol. 50, 569-602 (1994); (**I**) "Optimization of perfect and imperfect ring and stringer stiffened cylindrical shells with PANDA2 and evaluation of the optimum designs with STAGS", AIAA Paper 2002-1408, pp 1562-1613, Proceedings of the 43rd AIAA SDM Meeting, April, 2002, with C. Rankin; (**J**) "Optimum design of stiffened panels with substiffeners, AIAA Paper 2005-1932, AIAA 46th SDM Conference, April 2005, with C. Rankin; (**K**) "Difficulties in optimization of imperfect stiffened cylindrical shells, AIAA Paper 2006-1943, AIAA 47th SDM Conference, April 2006, with C. Rankin; (**L**).../panda2/doc/panda2.news, a continually updated file distributed with PANDA2 that contains a log of all significant modifications to PANDA2 from 1987 on.

[18] Almroth, B. O. and Brogan, F. A., "The STAGS computer code", NASA CR-2950, NASA Langley Research Center, Hampton, VA, 1978.

[19] STAGS Brochure (2002) available online by request: crankin@rhombuscgi.com (pdf format).

[20] (**A**) Rankin, C.C., Stehlin, P., and Brogan, F.A., "Enhancements to the STAGS computer code", NASA CR-4000, NASA Langley Research center, Hampton, VA, 1986. See also: (**B**) Rankin, C.C, "Application of Linear Finite Elements to Finite Strain Using Corotation." AIAA Paper AIAA-2006-1751, 47th AIAA Structures, Structural Dynamics and Materials Conference, May 2006; (**C**) Rankin, C.C., Brogan, F.A., Loden, W.A., Cabiness, H.D., "STAGS User Manual – Version 5.0," Rhombus Consultants Group, Inc., Palo Alto, CA, Revised January 2005 (on-line). Previously Report No. LMSC P032594, Lockheed Martin Missiles and Space Company, Palo Alto, CA, June 1998; (**D**) Rankin, C.C., "The use of shell elements for the analysis of large strain response, AIAA Paper 2007-2384, 48th AIAA Structures, Structural Dynamics and Materials Conference, Hawaii, April 2007.

[21] Riks, E., Rankin C. C., Brogan F. A., "On the solution of mode jumping phenomena in thin walled shell structures", First ASCE/ASM/SES Mechanics Conference, Charlottesville, VA, June 6-9, 1993, in: Computer Methods in Applied Mechanics and Engineering, Vol. 136, 1996.

The figures below are taken from various papers in which STAGS models play important roles.

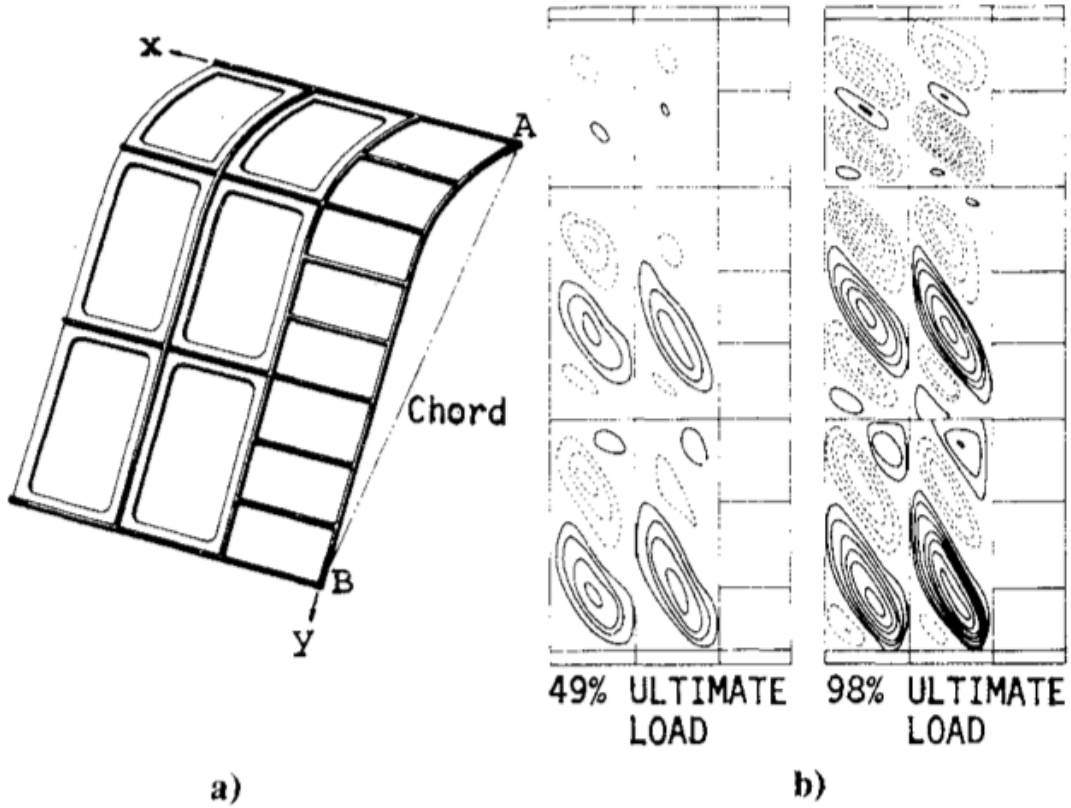

Fig. 6.7 Computer analysis of shear panel (from Skogh and Stern [151]), a) Complex stiffened shear panel, b) Post-buckling behavior predicted with the STAGS computer program. (Fig. 6.7 in "Pitfalls" paper, AIAA Journal, Vol. 19, No. 9, 1981). [151] Skogh, J. and Stern, P. "Post-buckling Behavior of a Section Representative of the B-l Aft Intermediate Fuselage," AFFDL-TTR-73-63, May 1973.

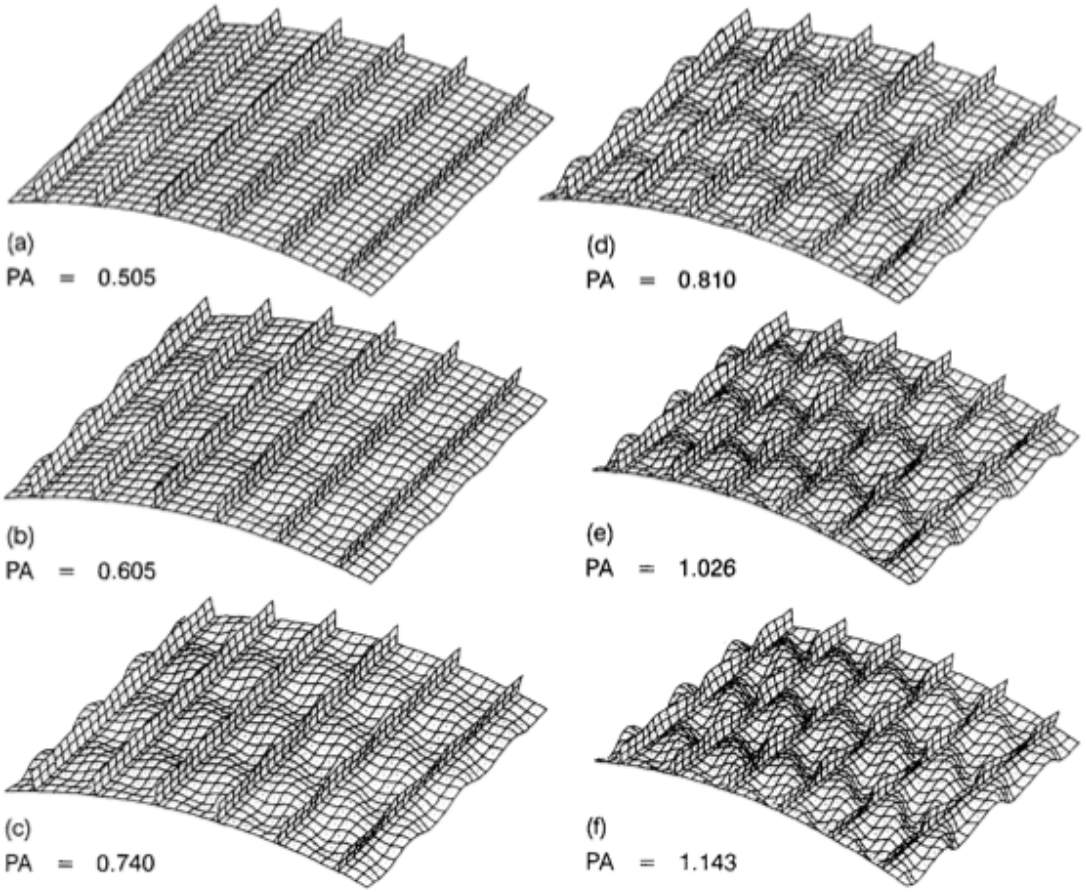

Fig. 42 State of the panel at various load factors, PA, for Load Set 3. PA = 1.0 is the design load (from Computer Methods in Applied Mechanics and Engineering, 103 (1993) 43-114)

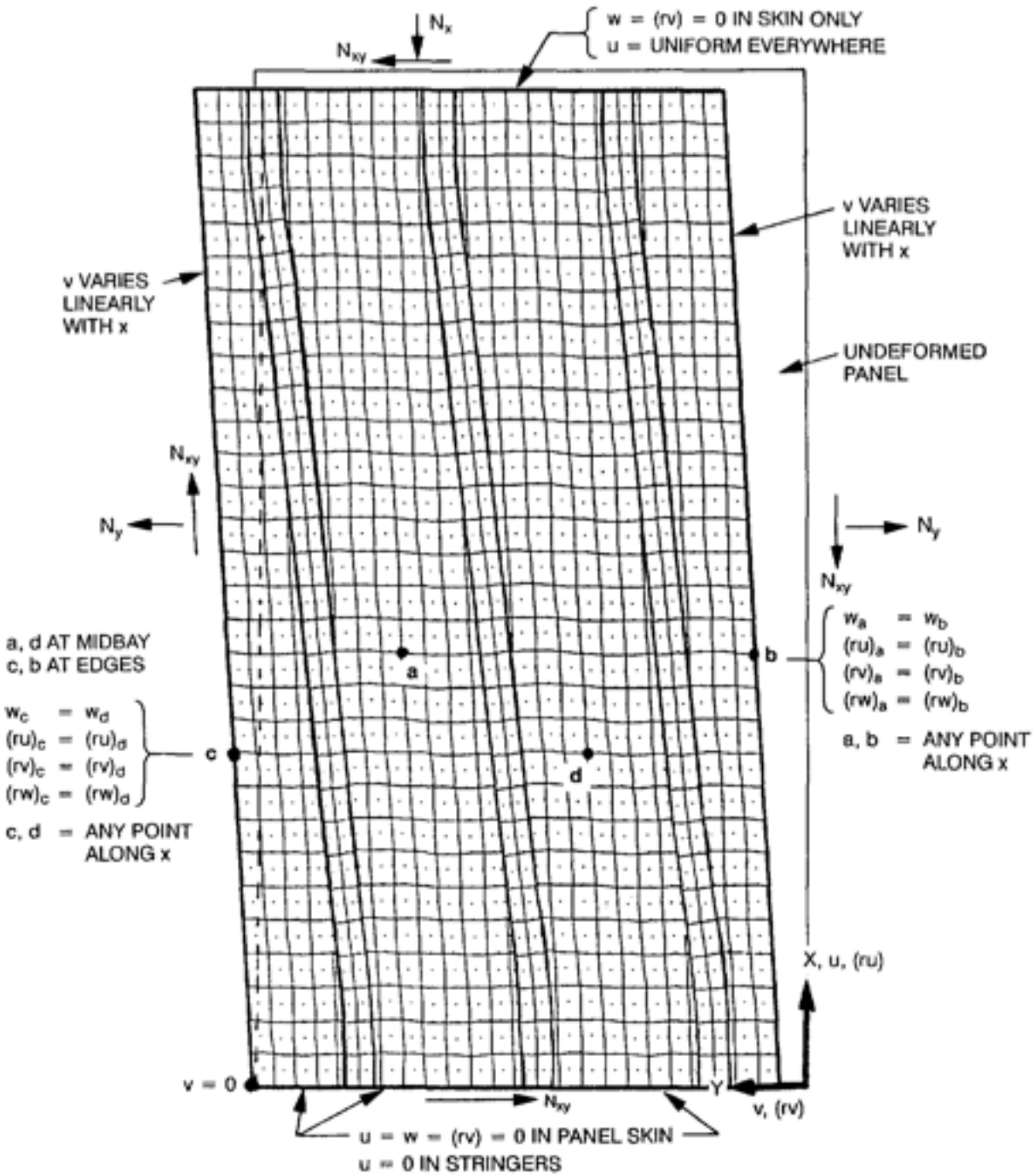

Fig. 25 Plan view of undeformed and deformed STAGS finite element model of the T-stiffened panel. The in-plane loading components, Nx and Nxy, are shown, as well as the boundary conditions for the case in which the two edges parallel to the stringers (longitudinal edges) are prevented from warping in the plane of the panel skin. (from Computers & Structures, Vol.55, No. 5, pp. 819-856, 1995)

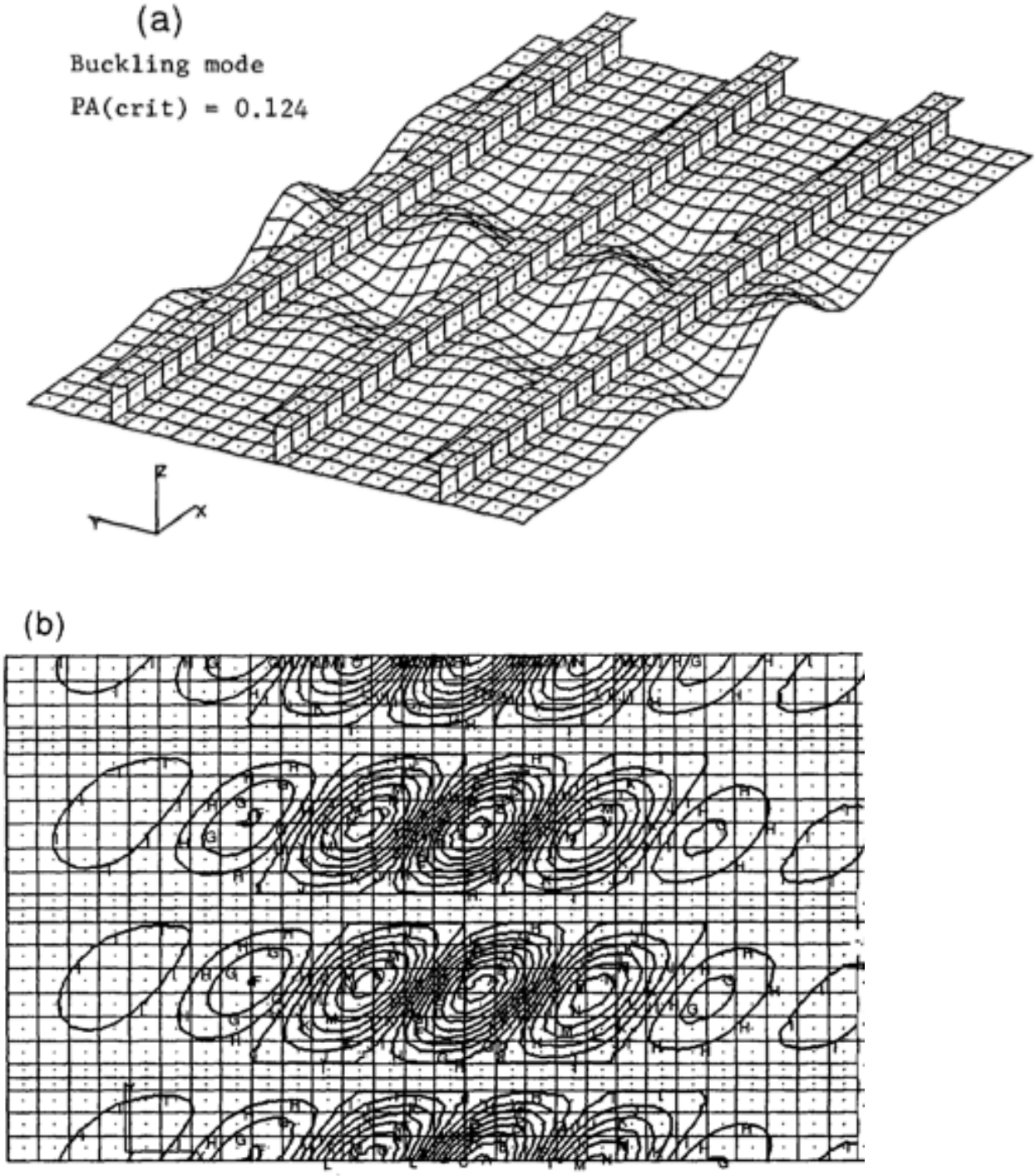

Fig. 26 STAGS prediction of buckling mode and critical load factor from linear bifurcation buckling theory. This mode shape is used as an initial imperfection in the nonlinear equilibrium STAGS analysis. (a) Three-dimensional view of buckling mode; (b) contour plot that shows the slope of the nodal lines of the local buckling mode and its axial wavelength. (from Computers & Structures, Vol.55, No. 5, pp. 819-856, 1995)

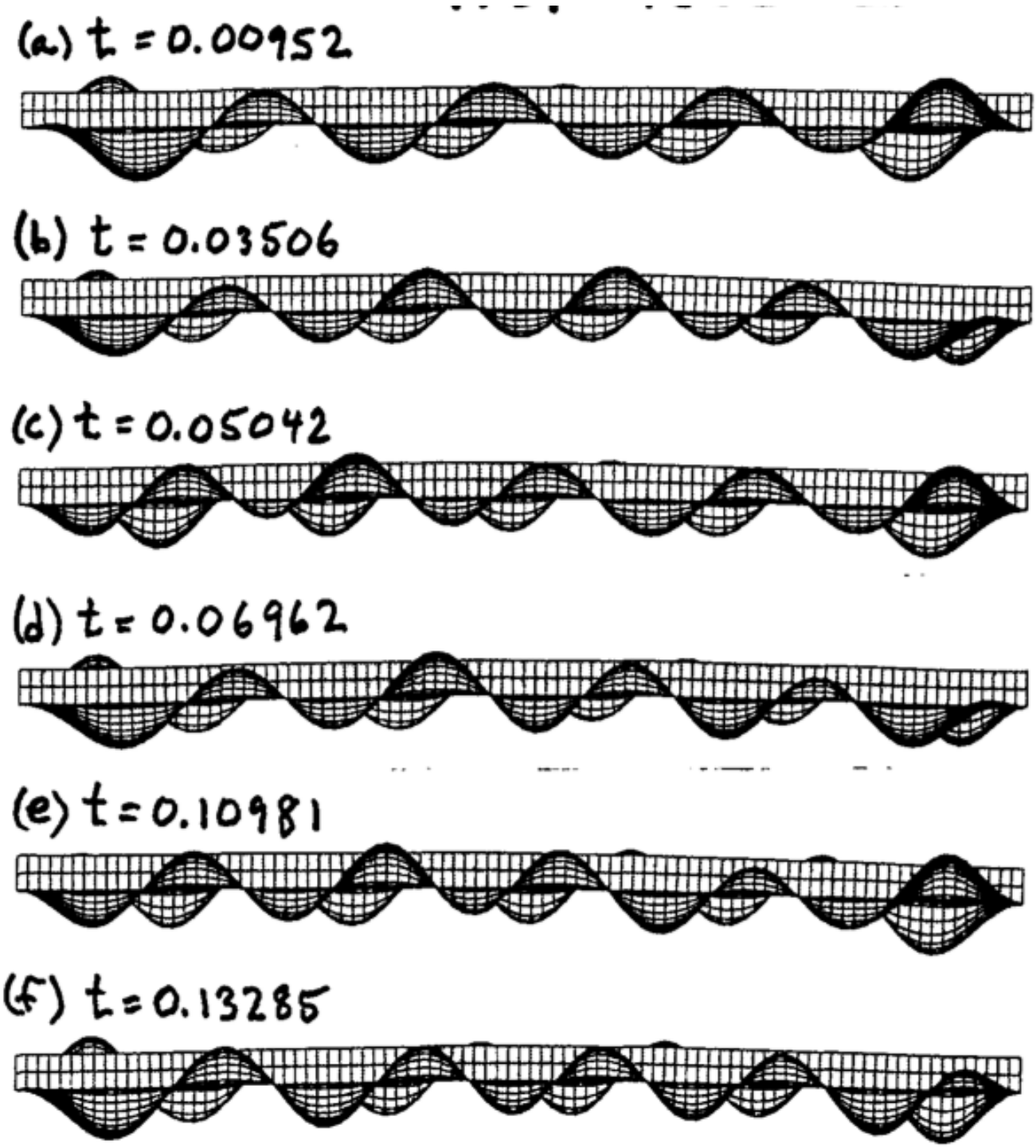

Fig. 29 Edge-on view of post-buckled PANEL I during transient phase at constant load factor, PA = 0.7013. Each frame corresponds to a peak value of hoop stress in the next figure.

From: AIAA 38th Structures, Structural Dynamics, and Materials Conference, AIAA Paper No. AIAA-97-1141, 1997

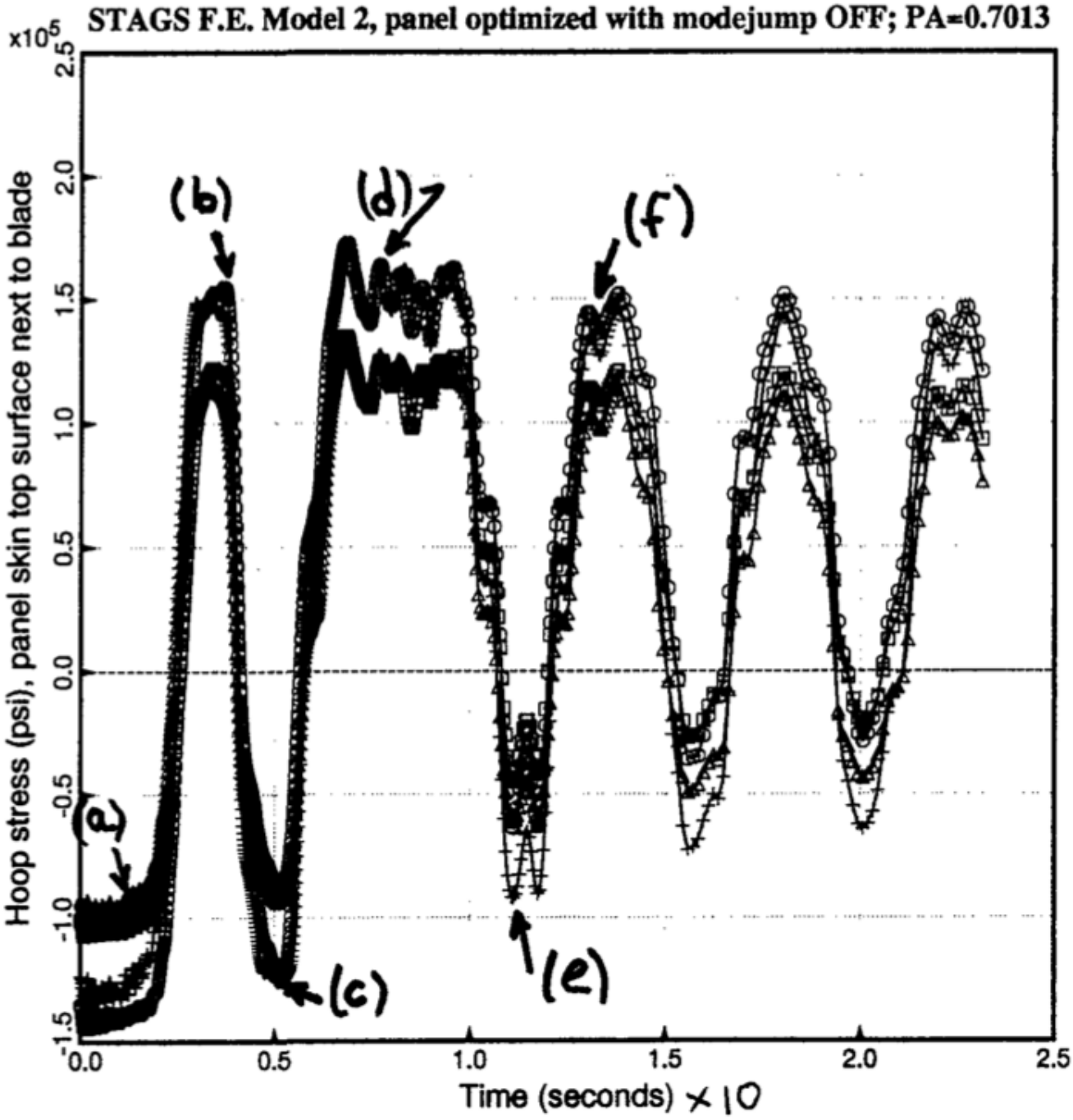

Fig. 30 Oscillations of the maximum hoop stress during the transient phase of the STAGS analysis (dynamic mode jump). The callouts, (a – f), refer to the "snapshots" in the previous figure.

From: AIAA 38th Structures, Structural Dynamics, and Materials Conference, AIAA Paper No. AIAA-97-1141, 1997

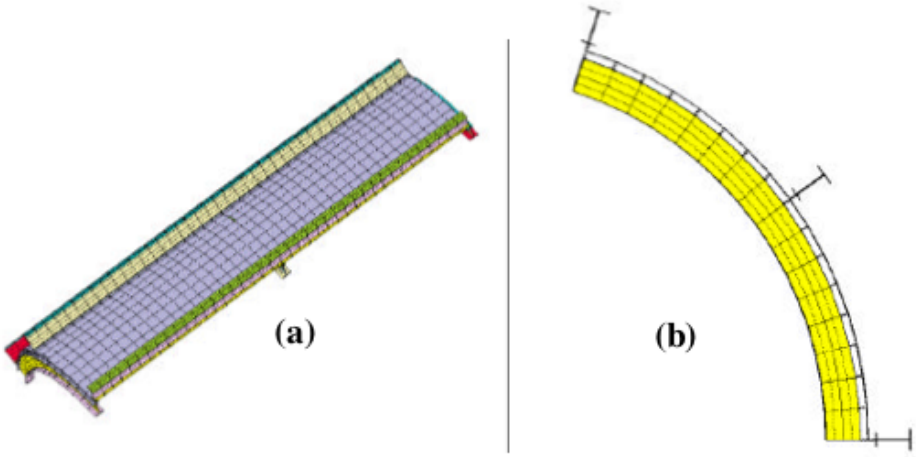

Fig. 1 STAGS model generated with STAGSUNIT for a starting design

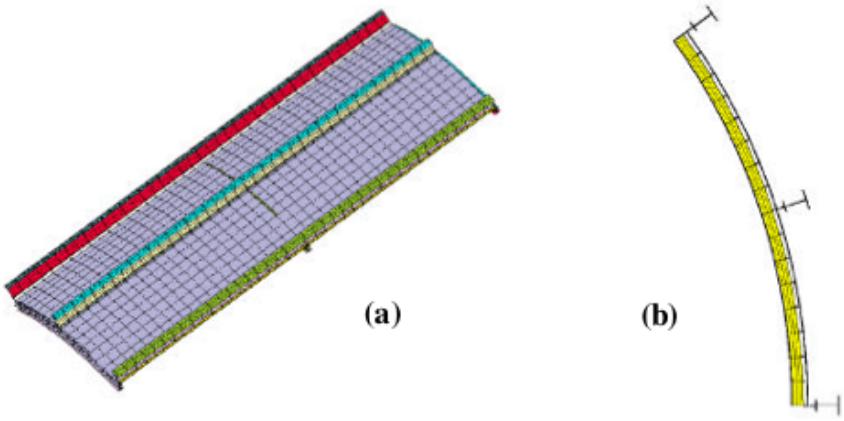

Fig. 2 STAGS model for the optimized design

Fig. 3 Bifurcation buckling of the optimized design under Load Set 1

From AIAA 43rd Structures, Structural Dynamics and Materials Conference, AIAA Paper 2002-1408

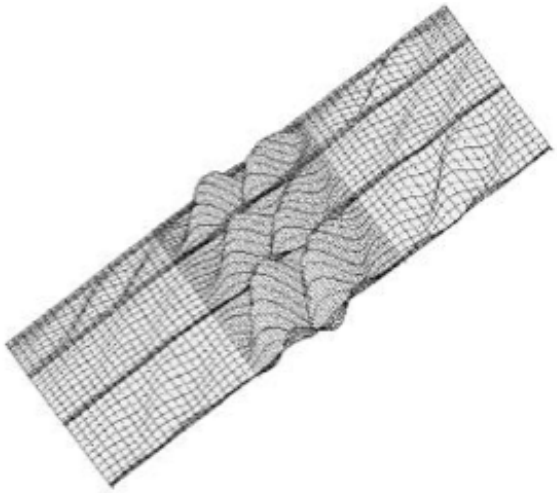

Fig. 17 Buckling of the skin in STAGS model type "2" for optimized perfect Blade stiffened shell

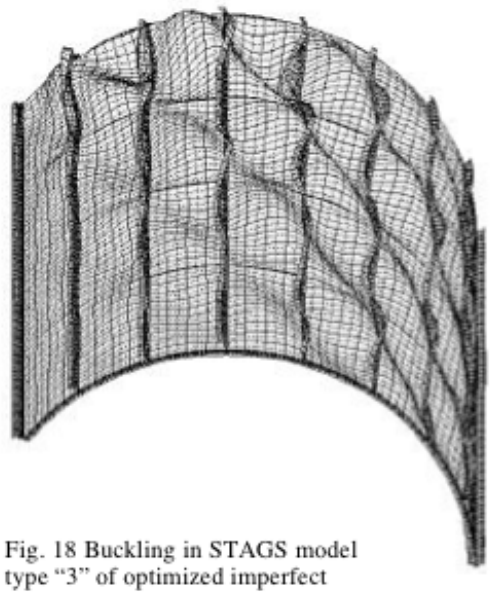

Fig. 18 Buckling in STAGS model type "3" of optimized imperfect Zee stiffened shell

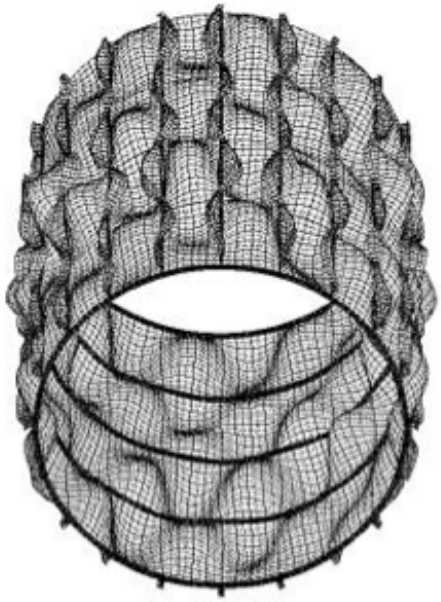

Fig. 19a Buckling in STAGS model type "4" of optimized imperfect Tee stiffened shell

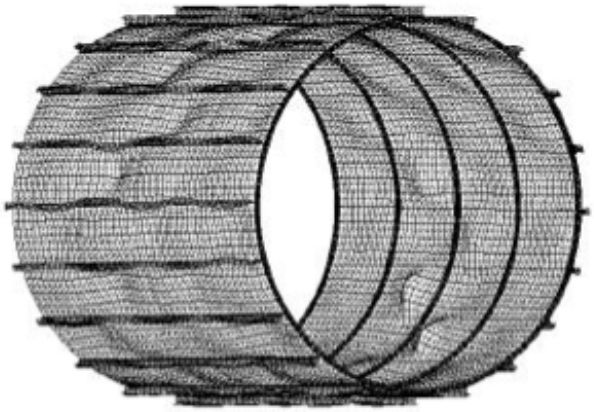

Fig. 19b Mode of collapse of the same shell as shown in Fig. 19a

From AIAA 43rd Structures, Structural Dynamics and Materials Conference, AIAA Paper 2002-1408

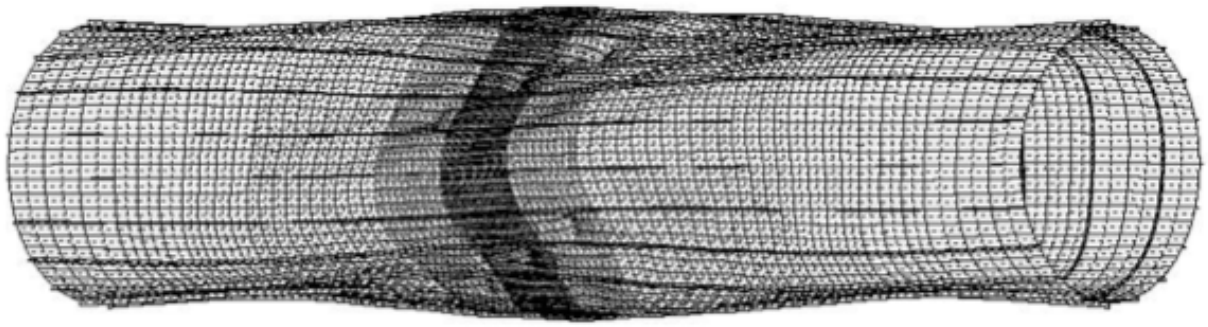

Fig. 27 Collapse mode in STAGS model type "5" for the optimized imperfect Blade stiffened shell

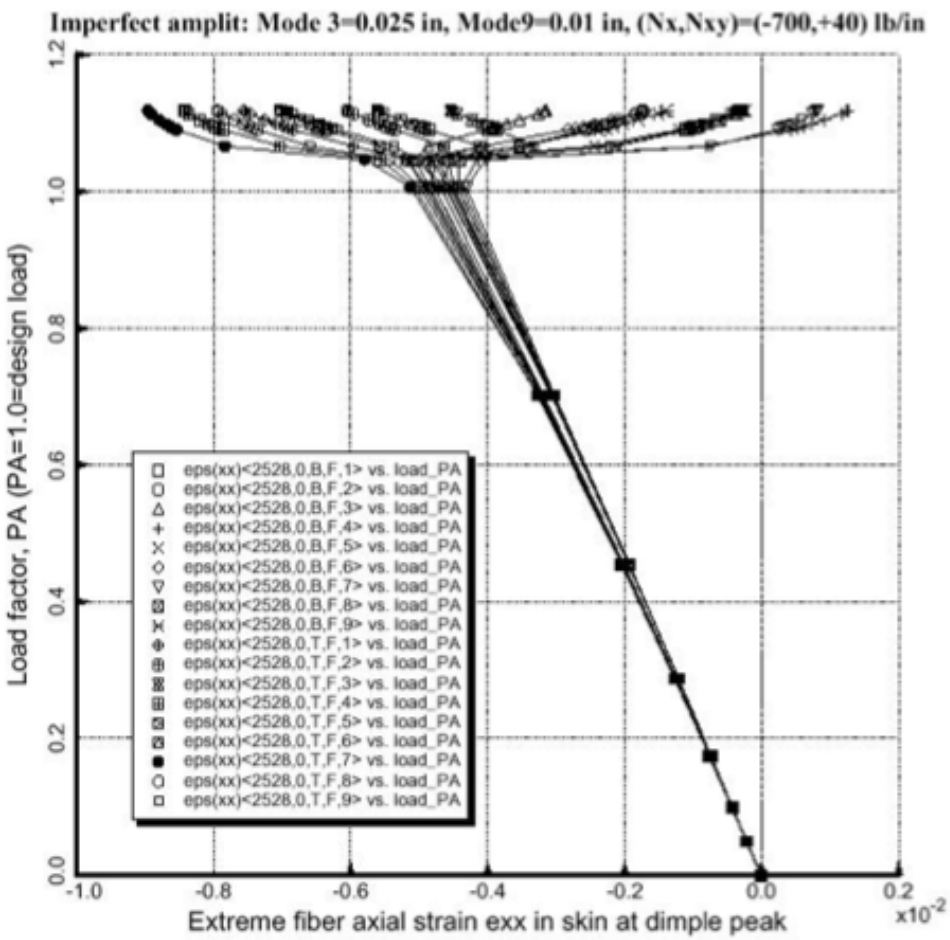

Fig. 28 Extreme fiber axial strain from the nonlinear STAGS analysis of the same shell shown in Fig. 27

From AIAA 43rd Structures, Structural Dynamics and Materials Conference, AIAA Paper 2002-1408

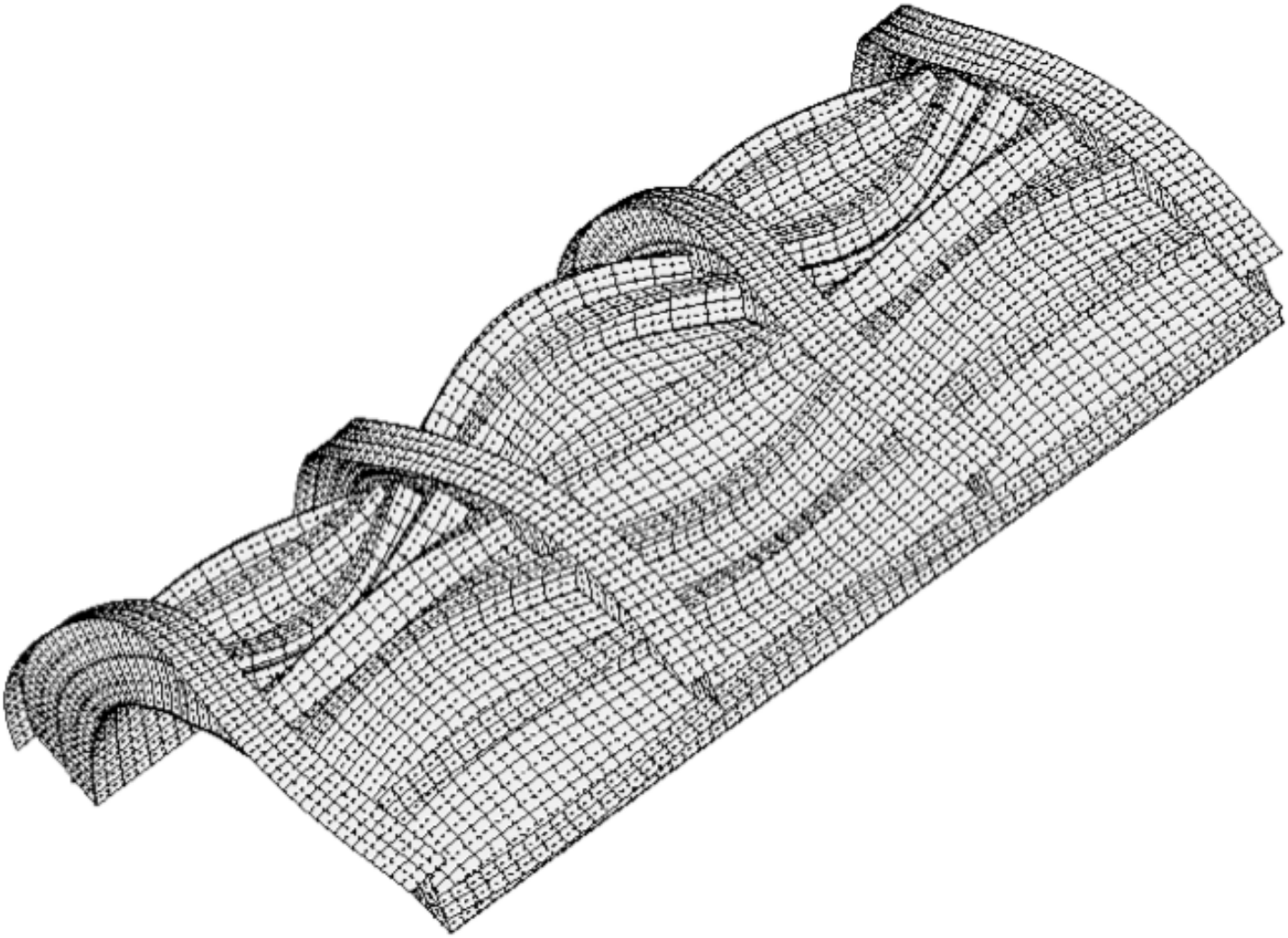

Fig. 5 STAGS model, 3 x nine bay, testax4p, sub-stiffeners are smeared, major stiffeners are shell units, STAGS 480 finite element, bifurcation buckling mode 1, buckling load factor, Pcr = 0.98903

From: AIAA 46th Structures, Structural Dynamics, and Materials Conference, Paper no. AIAA Paper 2005-1932, 2005

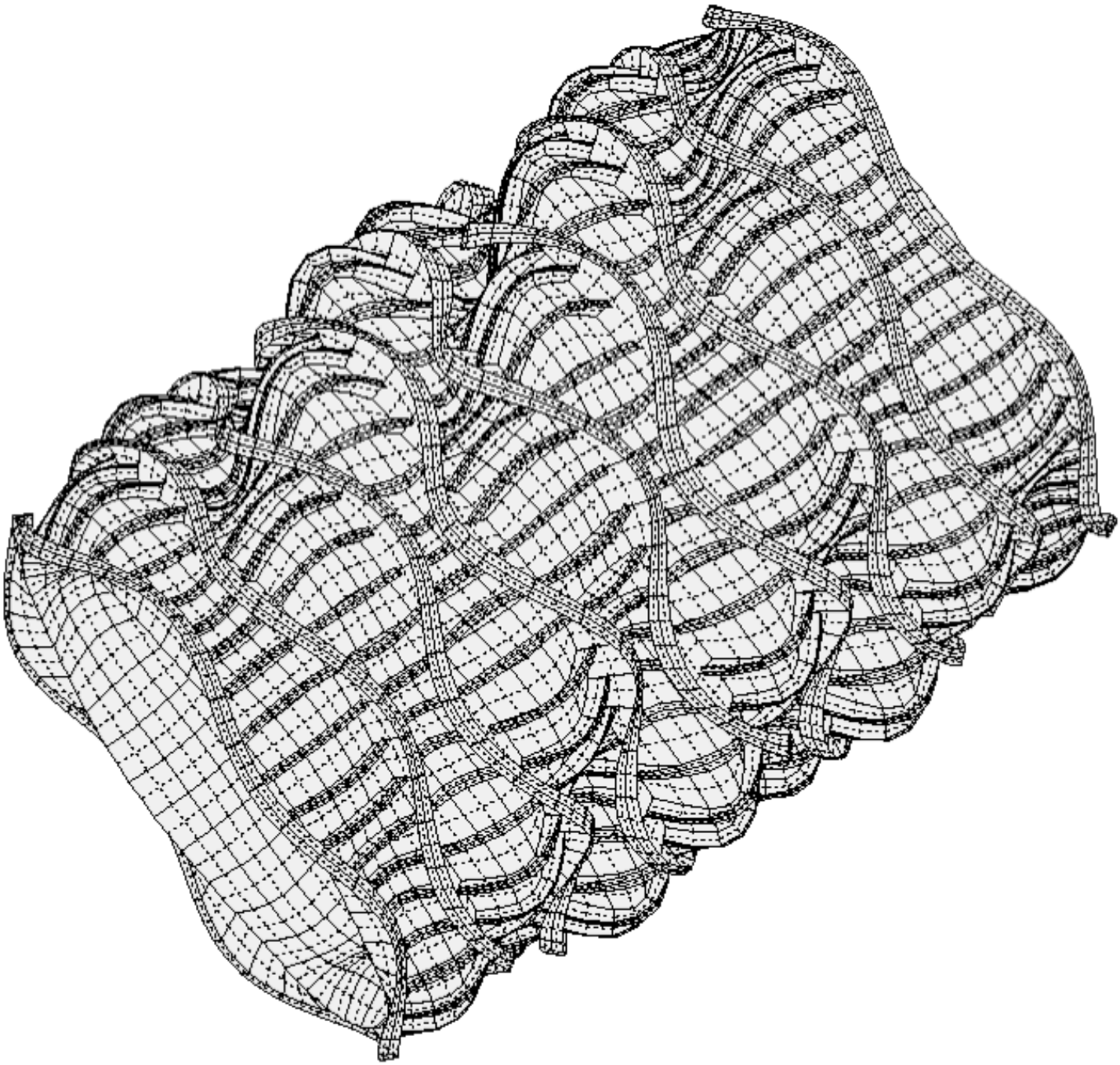

Fig. 6 STAGS model, entire shell testax4p, substiffeners are smeared, major stiffeners are shell units, the STAGS 480 finite element is used, bifurcation buckling mode 1, buckling load factor, Pcr = 1.0222

From: AIAA 46th Structures, Structural Dynamics, and Materials Conference, Paper no. AIAA Paper 2005-1932, 2005

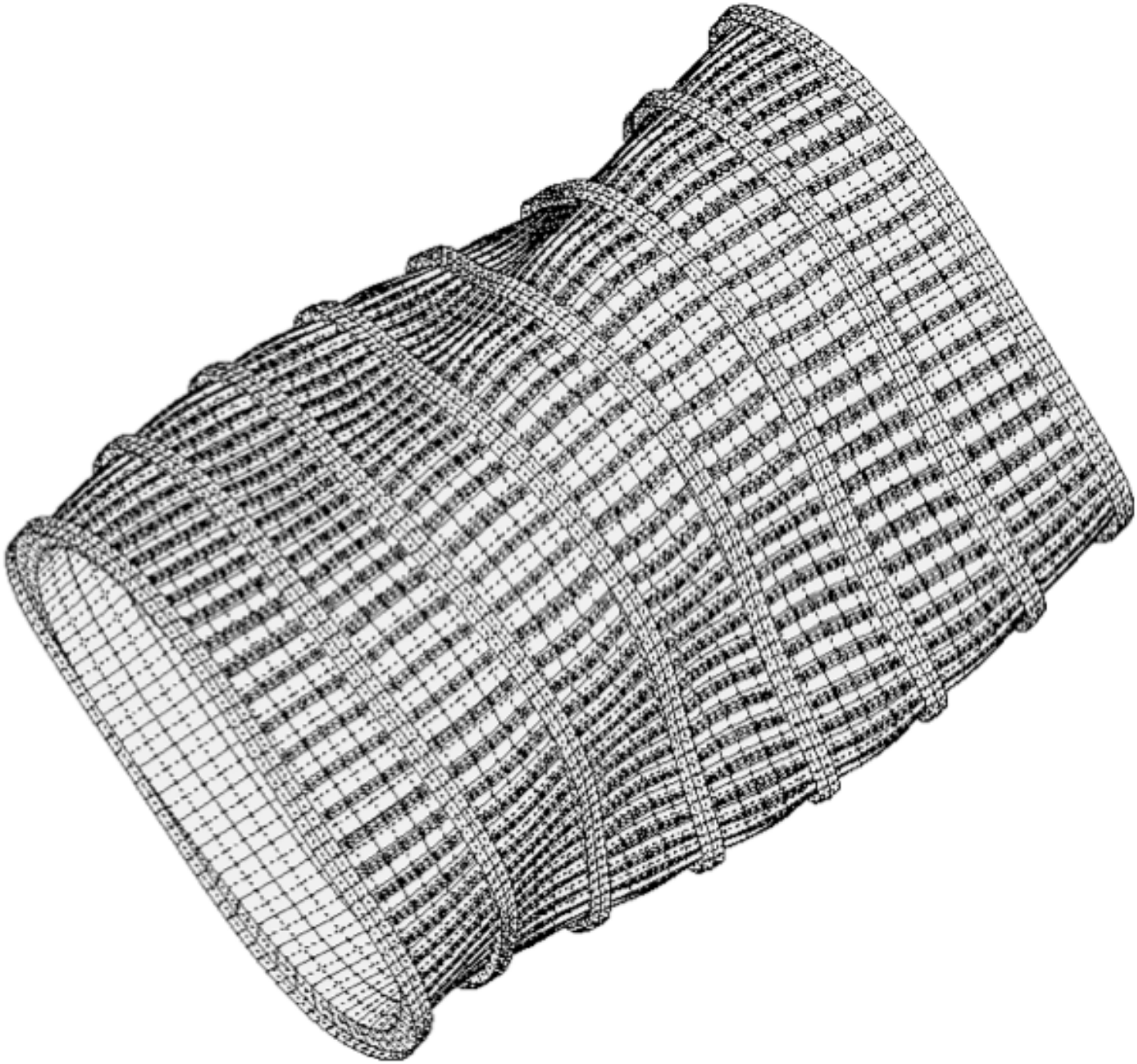

Fig. 15 STAGS model of the entire shell, testax4, sub-stiffeners are smeared, major stiffeners are shell units, the STAGS 480 finite element is used, bifurcation buckling mode 1, buckling load factor, Pcr = 1.4468

From: AIAA 46th Structures, Structural Dynamics, and Materials Conference, Paper no. AIAA Paper 2005-1932, 2005

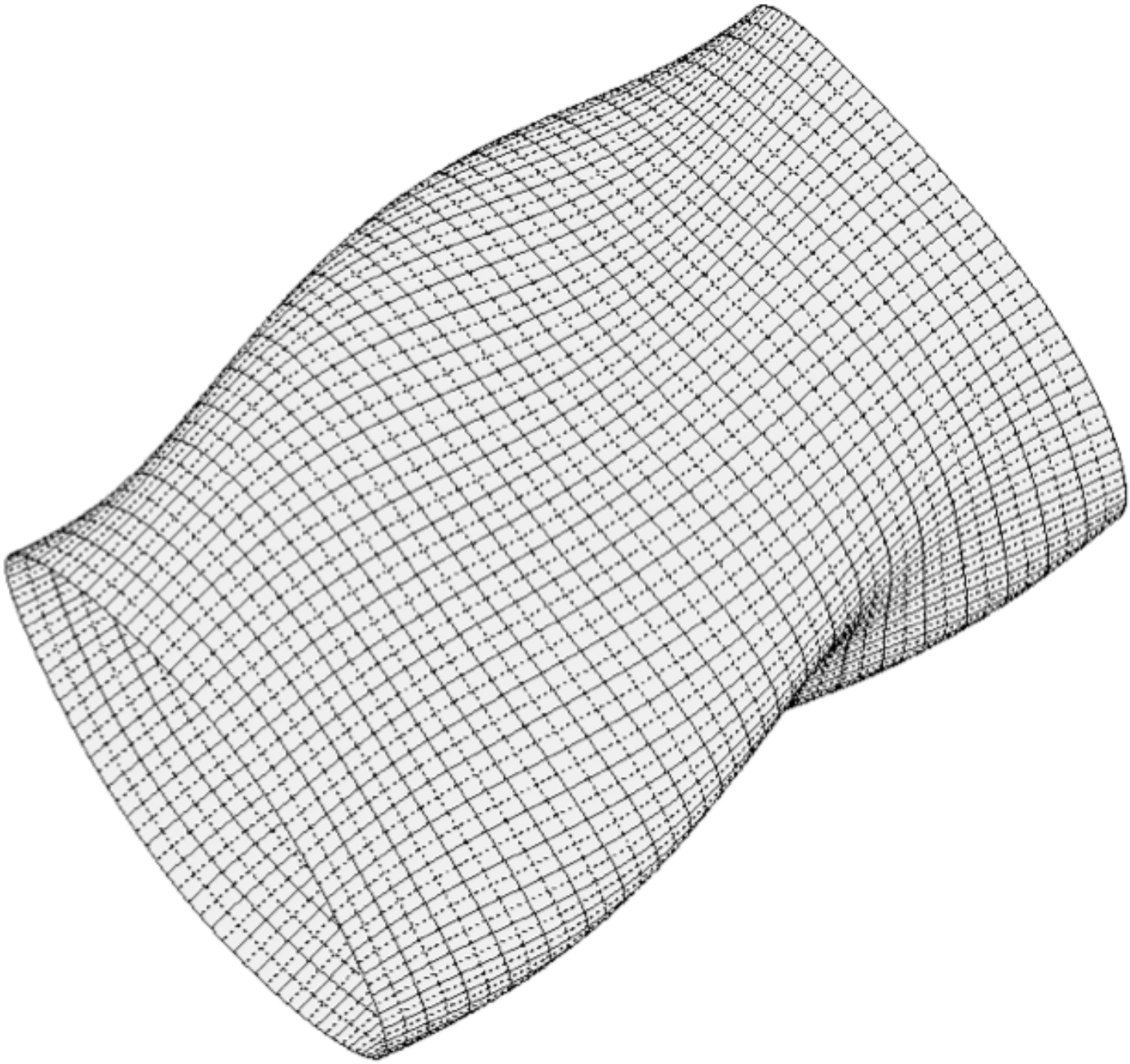

Fig. 16 STAGS model of the entire shell, testax4, all stiffeners are smeared, STAGS 480 finite element is used, bifurcation buckling mode 1, buckling load factor, Pcr = 1.8058

From: AIAA 46th Structures, Structural Dynamics, and Materials Conference, Paper no. AIAA Paper 2005-1932, 2005

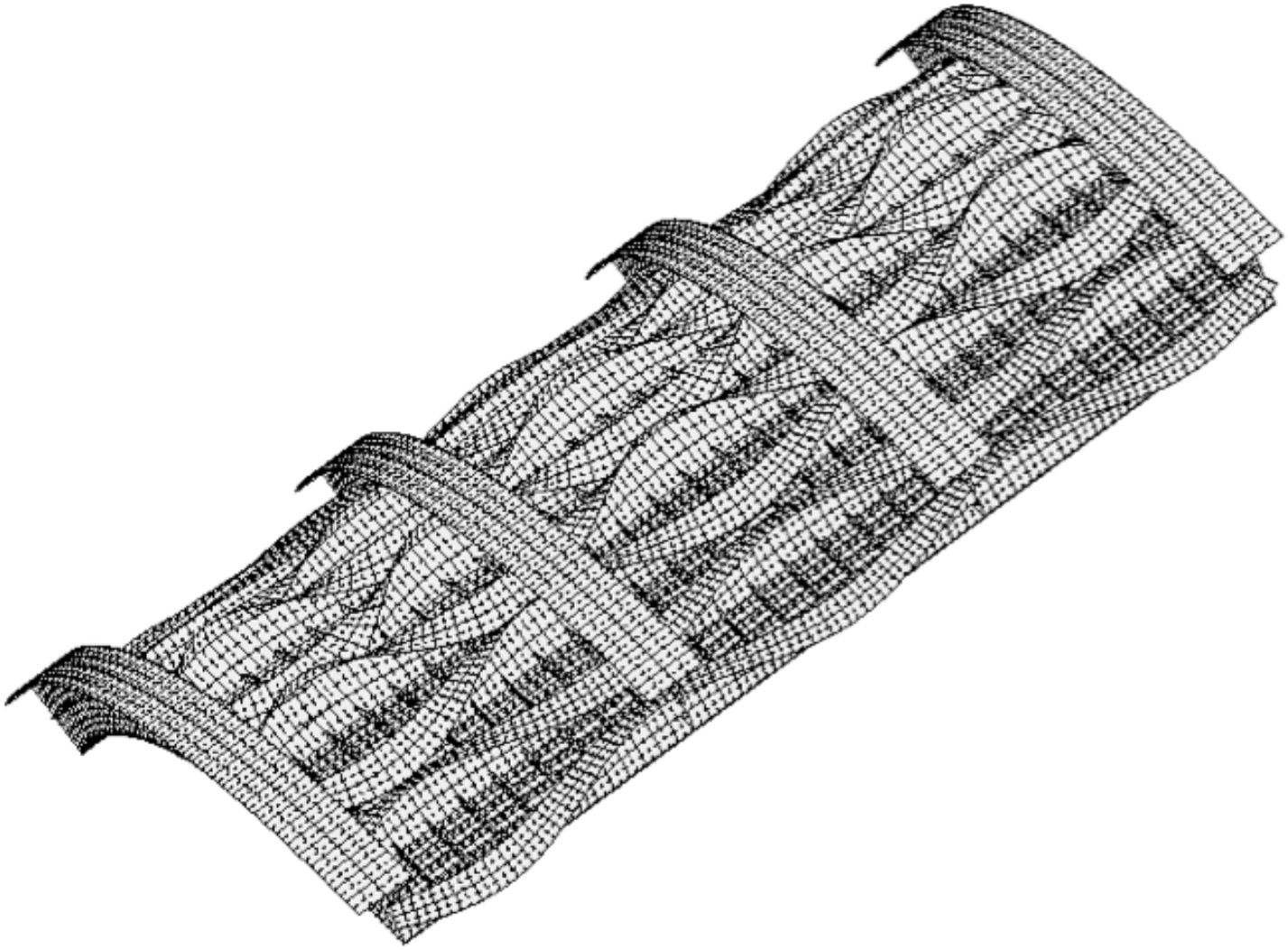

Fig. 17 STAGS model, 3 x 9 bays, testax4, all stiffeners are modeled as shell units, fasteners are used, the STAGS 480 finite element is used, this is bifurcation buckling mode 2, buckling load factor, Pcr = 1.2557

From: AIAA 46th Structures, Structural Dynamics, and Materials Conference, Paper no. AIAA Paper 2005-1932, 2005

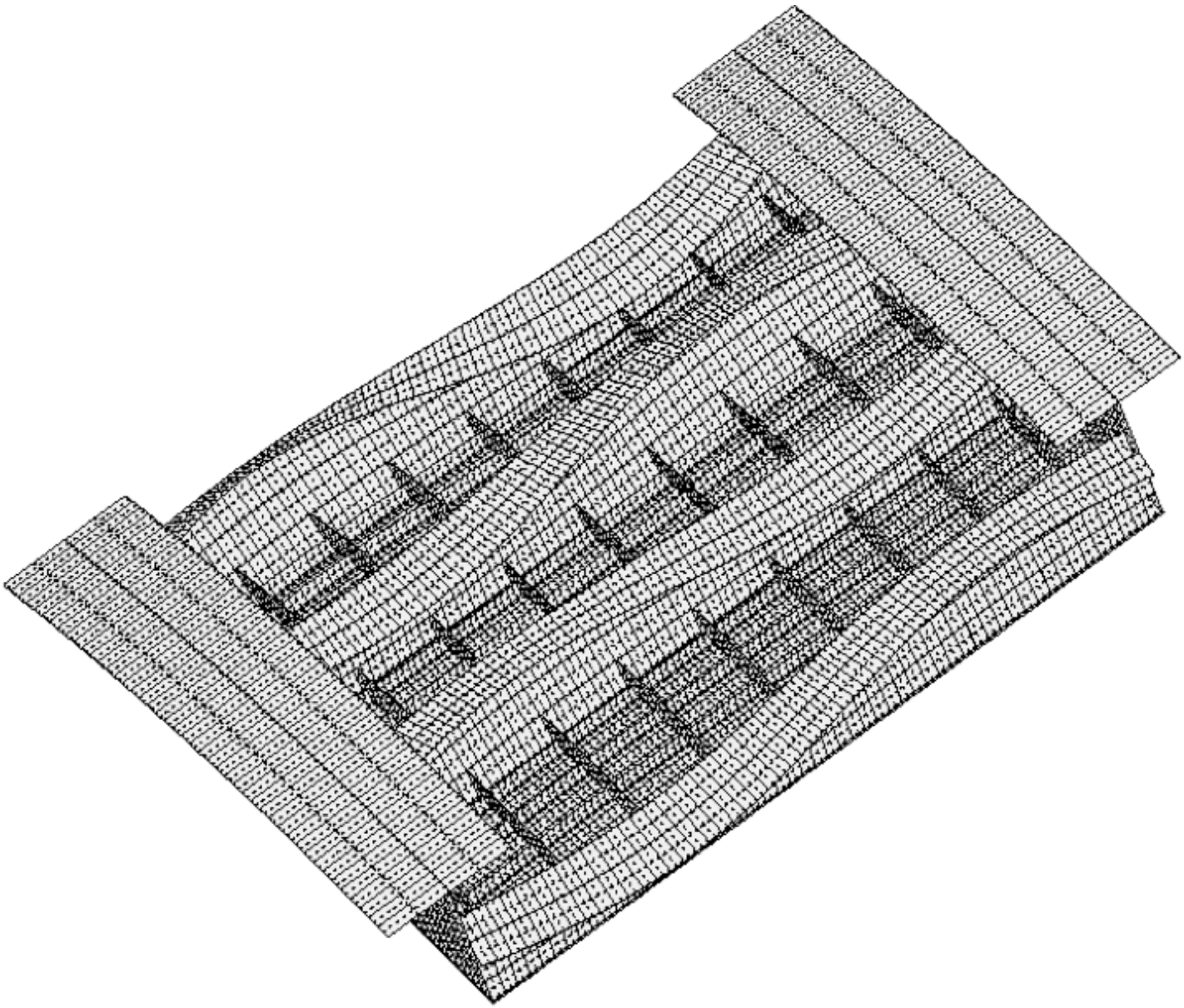

Fig. 18 STAGS inter-ring model, 1 x 3 major stiffener bays, all stiffeners are modeled as shell units, fasteners are used, the STAGS 480 finite element is used, bifurcation buckling mode 1, buckling load factor, Pcr = 1.2757

From: AIAA 46th Structures, Structural Dynamics, and Materials Conference, Paper no. AIAA Paper 2005-1932, 2005

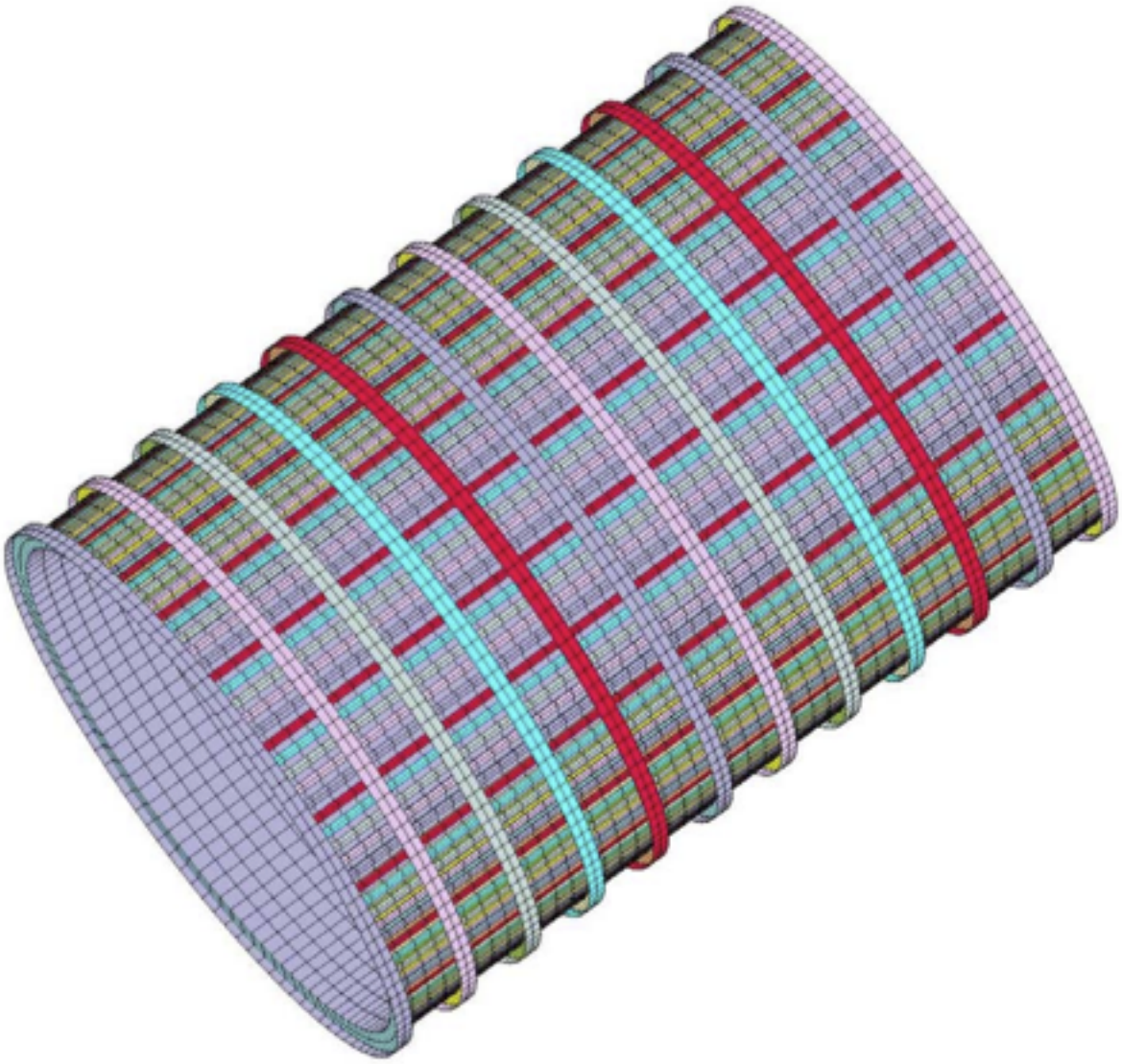

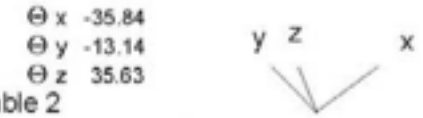

FIG. 1 STAGS model by STAGSUNIT; Entire cylindrical shell.
Case name = "testax3". The optimized shell configuration is listed in Table 2

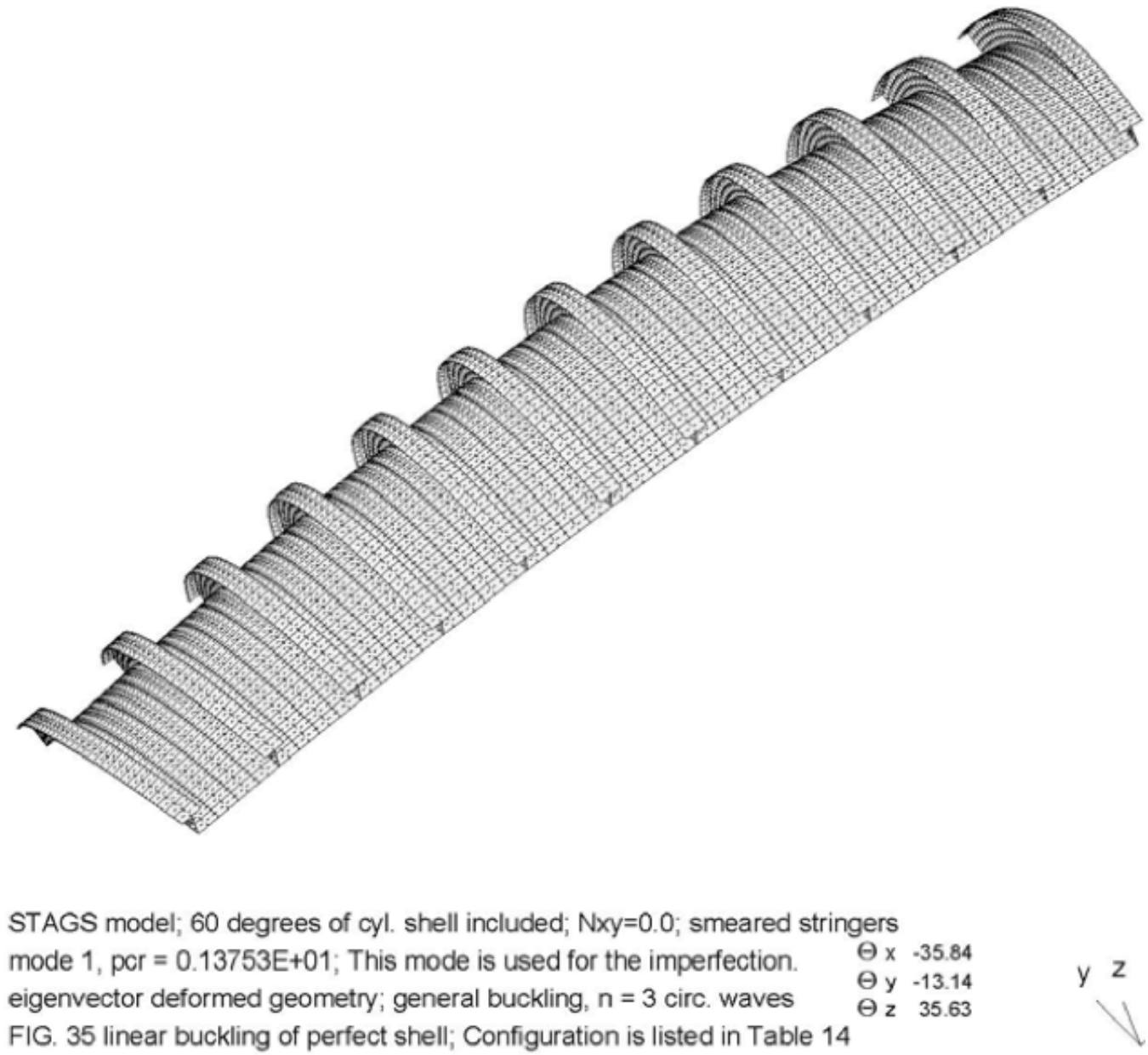

Fig. 35 STAGS model that includes 60 degrees of the cylindrical shell; shear resultant, Nxy = 0; stringers are smeared, the STAGS 480 finite element is used; linear buckling of the perfect shell; bifurcation buckling mode 1, buckling load factor = 1.3753; general buckling with n = 3 full circumferential waves over the full 360 degrees of the circumference of the cylindrical shell (one half circ. wave over the 60 degrees that are included in this model). This buckling mode is used as an initial imperfection. This configuration is listed in Table 14.

From: AIAA 47th Structures, Structural Dynamics, and Materials Conference, Paper no. AIAA-2006-1943, 2006

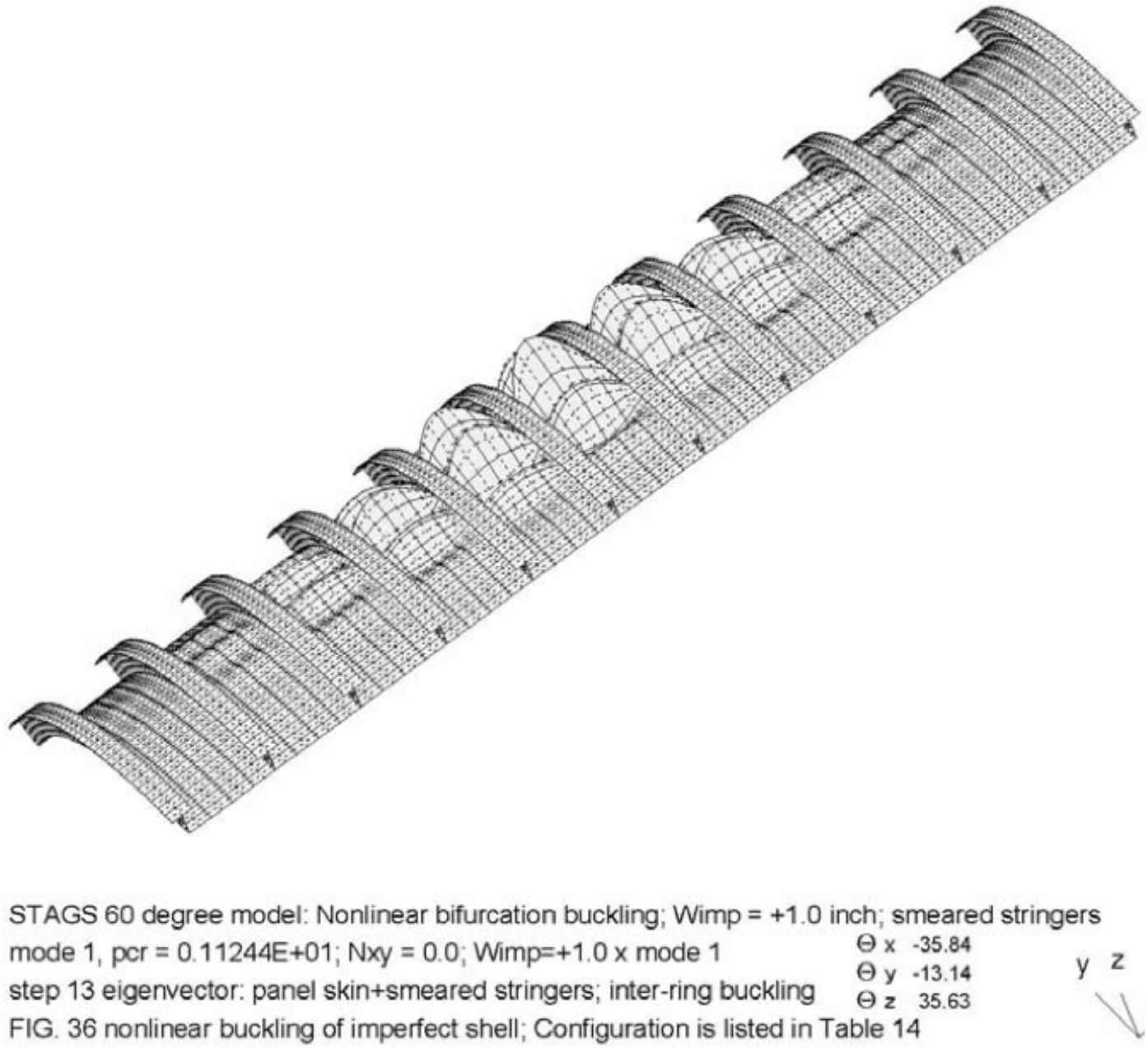

Fig. 36 STAGS model that includes 60 degrees of the cylindrical shell; shear resultant, Nxy = 0; stringers are smeared, the STAGS 480 finite element is used; nonlinear buckling of the imperfect shell; general buckling modal imperfection amplitude, Wimp = 1.0 inch; the imperfection shape is shown in the previous figure; nonlinear bifurcation buckling mode 1; buckling load factor = 1.1244; the buckling mode is inter-ring buckling. This configuration is listed in Table 14.

From: AIAA 47th Structures, Structural Dynamics, and Materials Conference, Paper no. AIAA-2006-1943, 2006

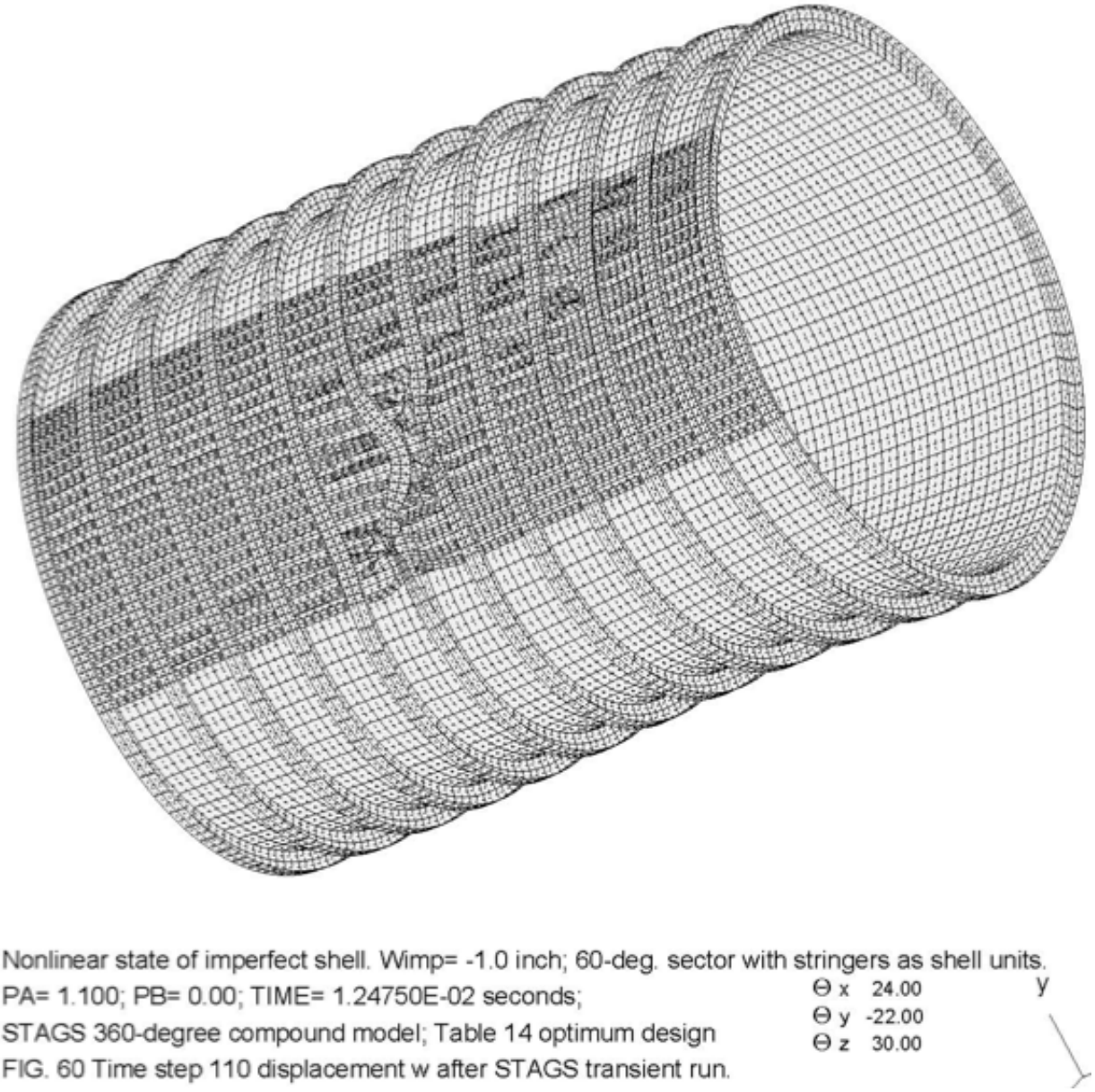

Fig. 60 STAGS compound model of the optimum design obtained from PANDA2 (Table 14) for the externally T-ring and T-stringer stiffened imperfect cylindrical shell; general buckling modal imperfection with amplitude, Wimp = -1.0 inch. The stringers are modeled as shell units over a 60-degree sector and are smeared out over the remaining 300 degrees of circumference. This figure shows the nonlinearly deformed state of the imperfect shell at load factor PA = 1.100 and at TIME = 0.012475 seconds (time step no. 110) during an execution of STAGS with INDIC = 6 (STAGS transient run). PA = 1.0 corresponds to the design load under which the shell was previously optimized by PANDA2.

From: AIAA 47th Structures, Structural Dynamics, and Materials Conference, Paper no. AIAA-2006-1943, 2006

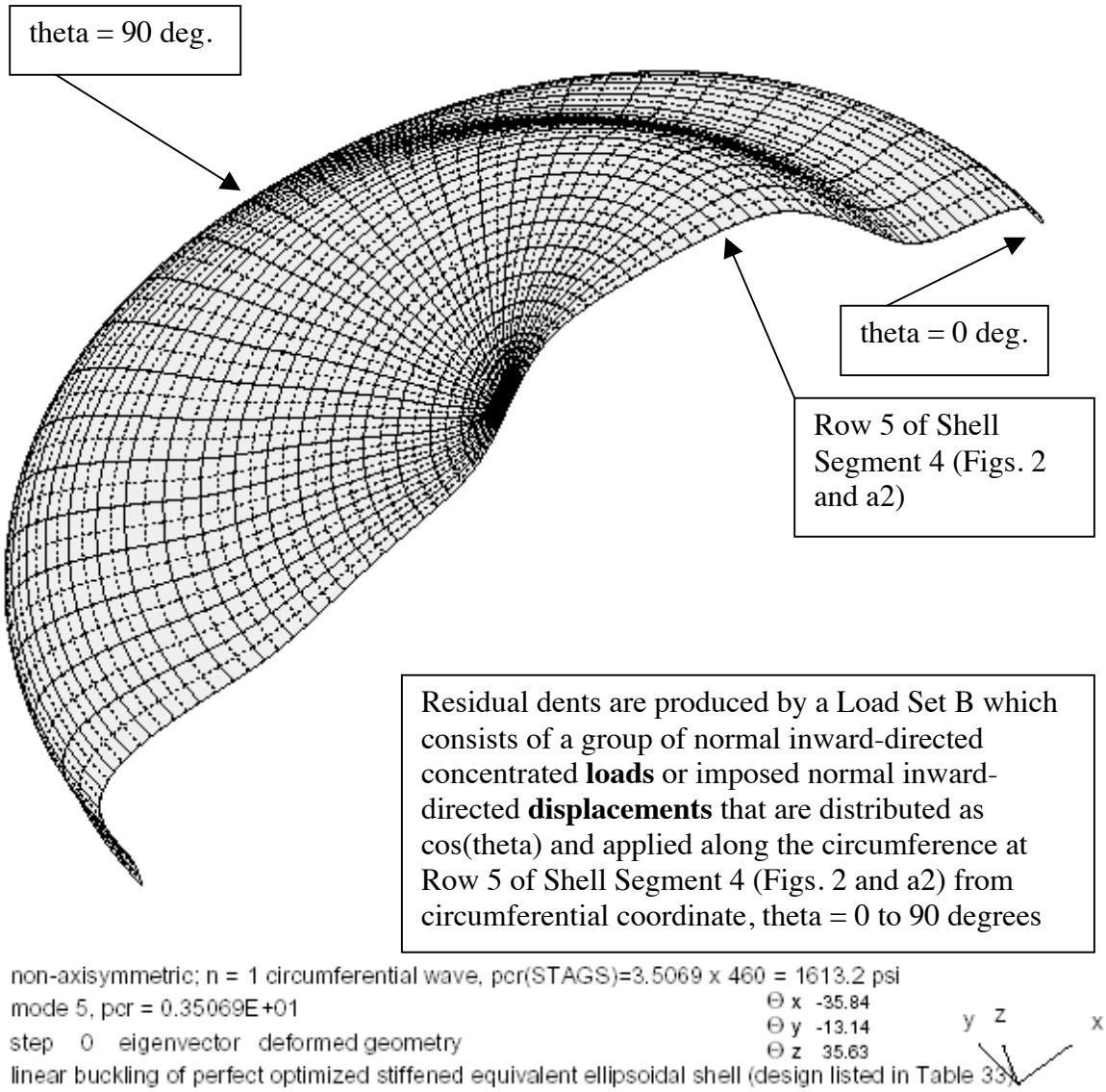

Fig. 262 **STAGS "soccerball" model of the optimized imperfect isogrid-stiffened equivalent ellipsoidal shell. The optimum design, listed in columns 2 and 3 of Table 33, was obtained with plus and minus axisymmetric (n=0) mode 1 and mode 2 linear buckling modal imperfection shapes with amplitude, Wimp = 0.2 inch.** This is the non-axisymmetric (2nd n=1 circumferential wave) linear buckling modal imperfection shape used as the n = 1 imperfection corresponding to the last trace in Fig. 254. Compare with the 360-degree STAGS model displayed in Fig. 10. The difference in the eigenvalue, 3.5069 here vs 3.5518 in Fig. 10, is caused primarily by the difference in the finite element used in the STAGS model: STAGS Element 480 here vs STAGS Element 410 in Fig. 10. Indicated in this figure is the location where normal inward-directed concentrated loads or displacements are imposed in a "cos(theta)" distribution in order to produce a dent that **locally** resembles the negative of this linear buckling mode shape.

Presented at: AIAA 50th Structures, Structural Dynamics, and Materials Conference, Palm Springs, California, 2009, AIAA Paper 2009-2702

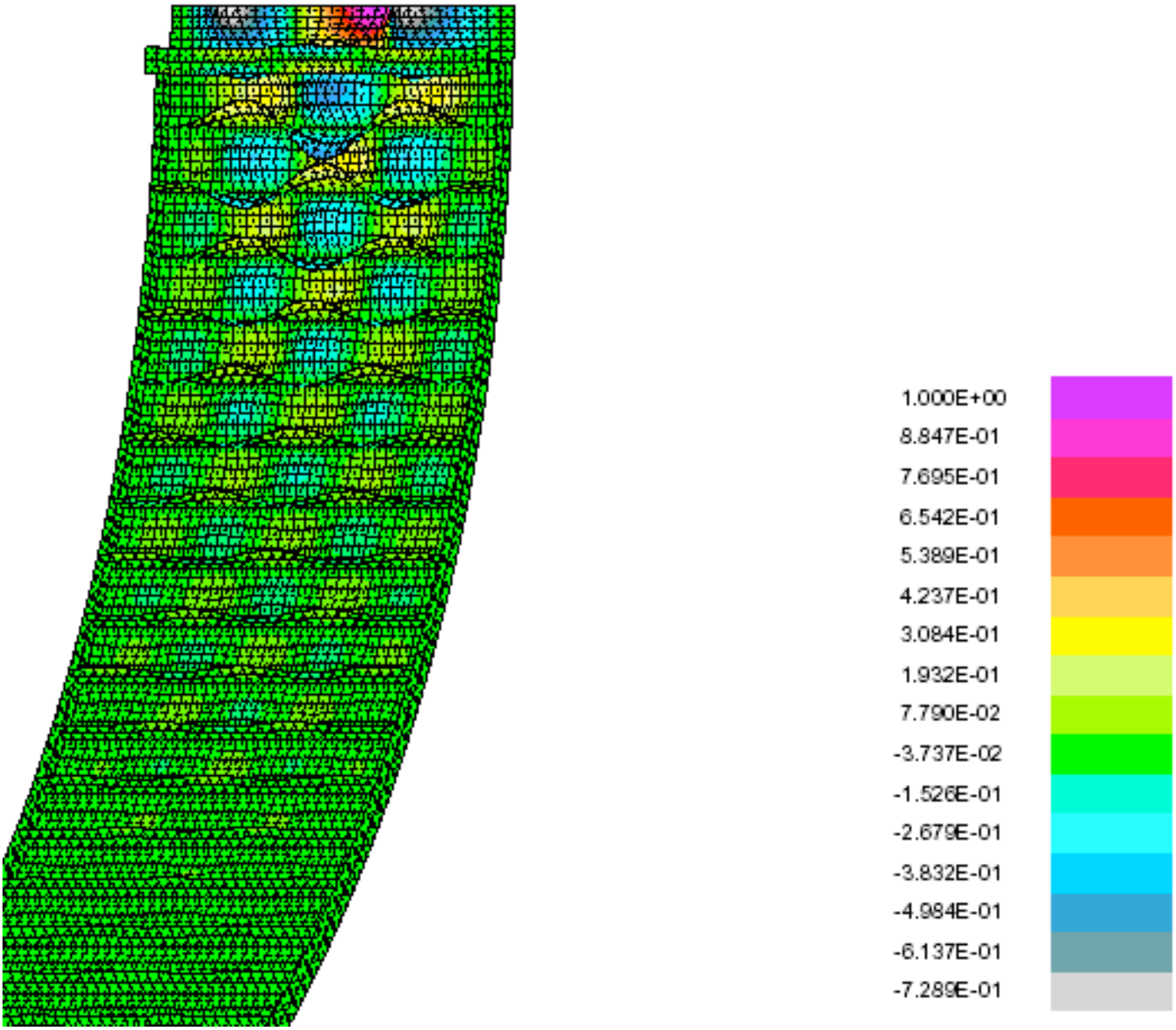

Fig. 27 STAGS "60-degree", one-ring-bay model. This is the same buckling mode as that shown in the previous two figures.

Presented at: AIAA 51st Structures, Structural Dynamics, and Materials Conference, 2010, AIAA Paper 2010-2927

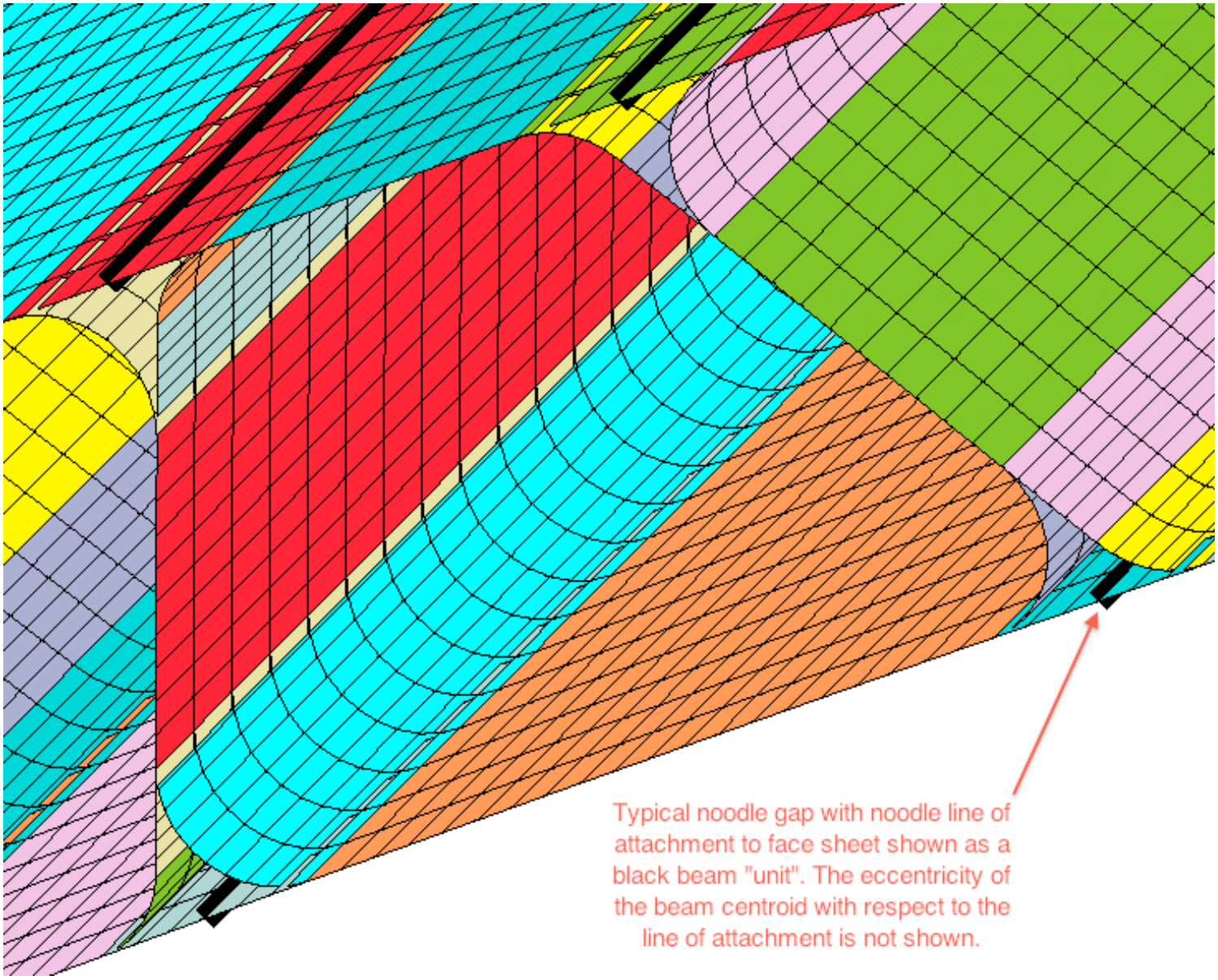

Fig. 18 "**nasatruss2**" starting design (Table 3). **Close-up view of a STAGS finite element model of one of the local buckling modules.** Each shell unit is shown in a different color. The black "units" represent the noodles. Unfortunately, STAGS does not show the eccentricity of the noodle centroid with respect to its attachment point of the face sheet. However, this eccentricity is present and accounted for in the STAGS model. The STAGS input file, *.inp, is automatically created by the generic GENOPT/BIGBOSOR4 case called "**trusscomp**". Comparisons between results from GENOPT/BIGBOSOR4 and general purpose computer programs such as STAGS [15-18] are provided in [1].

Presented at: AIAA 52nd Structures, Structural Dynamics, and Materials Conference, 2011, AIAA Paper 2011-1811

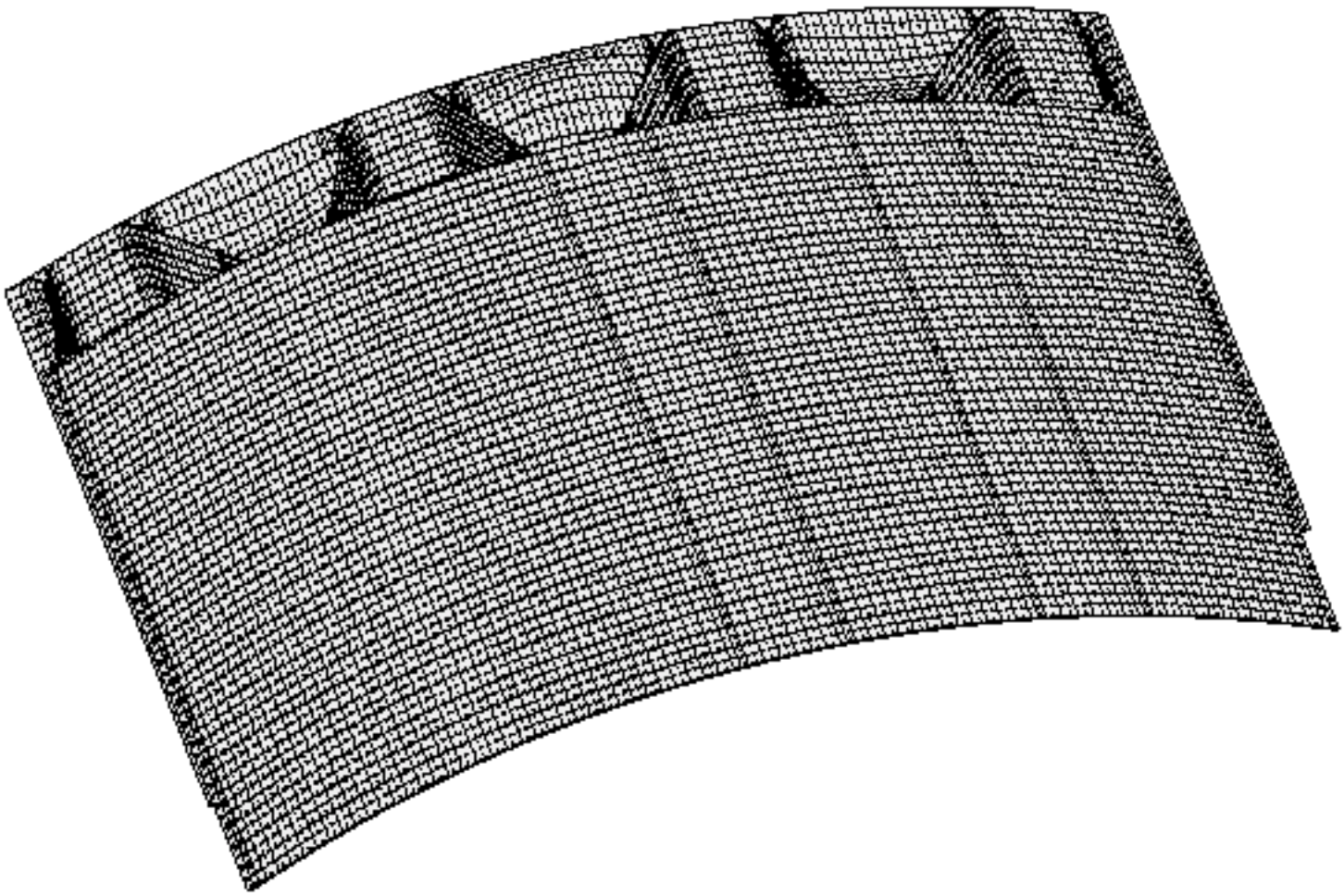

Fig. 19 A typical local buckling mode from a STAGS model of part of the axially compressed truss-core sandwich cylindrical shell. The axial length included in this model is FACLEN x LENGTH = 0.05 x 109 = 5.45 inches. Four 22- segment modules of the type shown in Fig. 4 are included in this particular local buckling model. “Noodles” and “noodle gaps” are included in this model. The STAGS 480 finite element is used for the shell segments and the STAGS 928 finite elements are used for the “noodles”, which are treated as discrete stringers located in the “noodle gaps” (Fig. 18). This particular STAGS model has a much smaller radius (7.815 inches) than the radius (78.15 inches) of the cylindrical shell that is the subject of the rest of this paper. The much smaller radius is used in this figure so that the reader can easily see that the STAGS model for local buckling includes the overall curvature of the cylindrical shell. The axial compression is applied by uniform end shortening in such a way that the pre-buckled state of the shell is uniform axial compression with only very small localized edge effects that do not affect the buckling behavior (Fig. 1g).

Presented at: AIAA 52nd Structures, Structural Dynamics, and Materials Conference, 2011, AIAA Paper 2011-1811

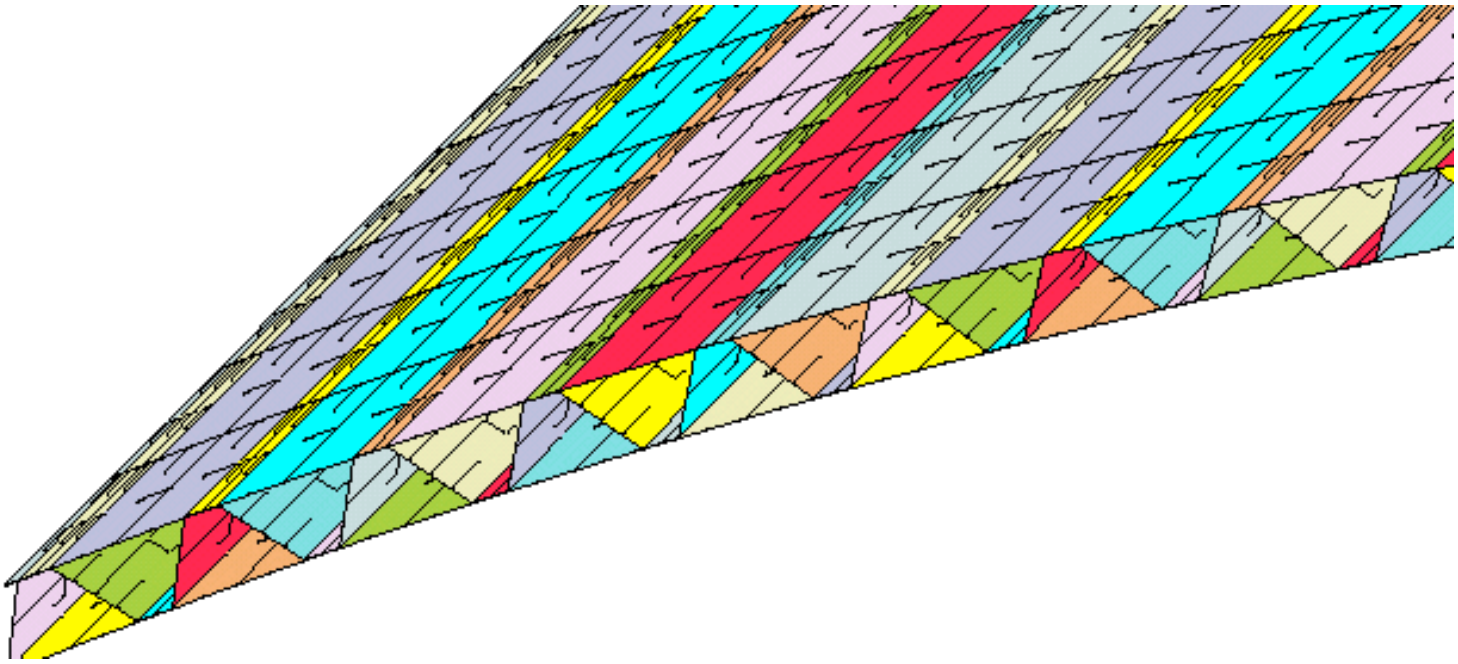

Fig. 20b "**nasatruss2**" starting design (Table 3). Detail from the lower left-hand corner of the previous figure. This model has two 480 finite elements (NCOLSG = 5) across the width of each of the six segments in each module of the 46-module general buckling model. A single module in this STAGS multi-module model is analogous to the GENOPT/BIGBOSOR4 module shown at the top of Fig. 6.

Presented at: AIAA 52nd Structures, Structural Dynamics, and Materials Conference, 2011, AIAA Paper 2011-1811

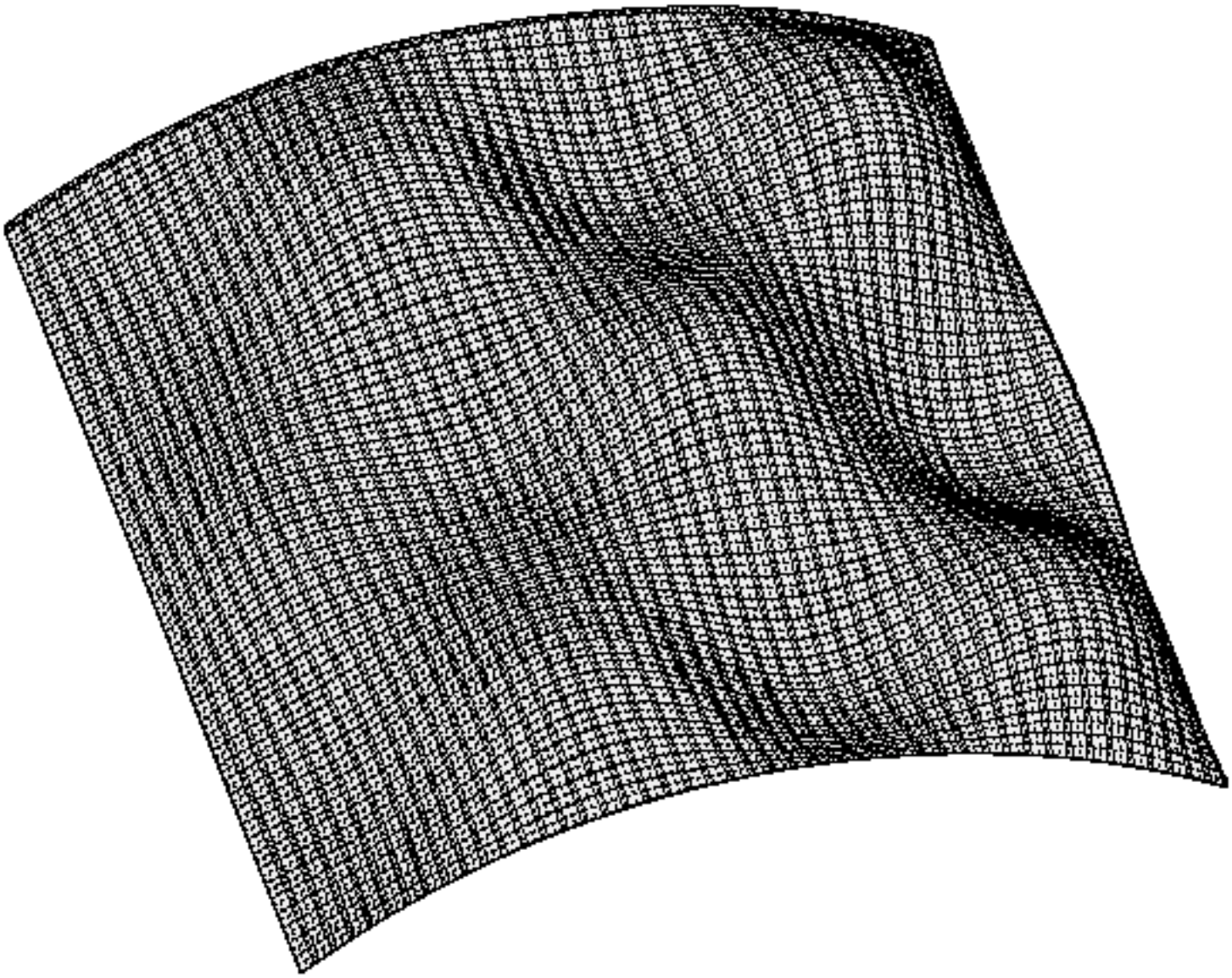

Fig. 21 "**nasatruss2**" starting design (Table 3). A general buckling mode from the STAGS model displayed in the previous two figures. The STAGS 480 finite element is used for the shell segments, and the STAGS 928 finite element is used for the noodles, which are represented as discrete stringers. The noodles are not shown in this figure.

Presented at: AIAA 52nd Structures, Structural Dynamics, and Materials Conference, 2011, AIAA Paper 2011-1811

From: AIAA 48th Structures, Structural Dynamics, and Materials Conference, Paper no. AIAA-2007-2216, 2007

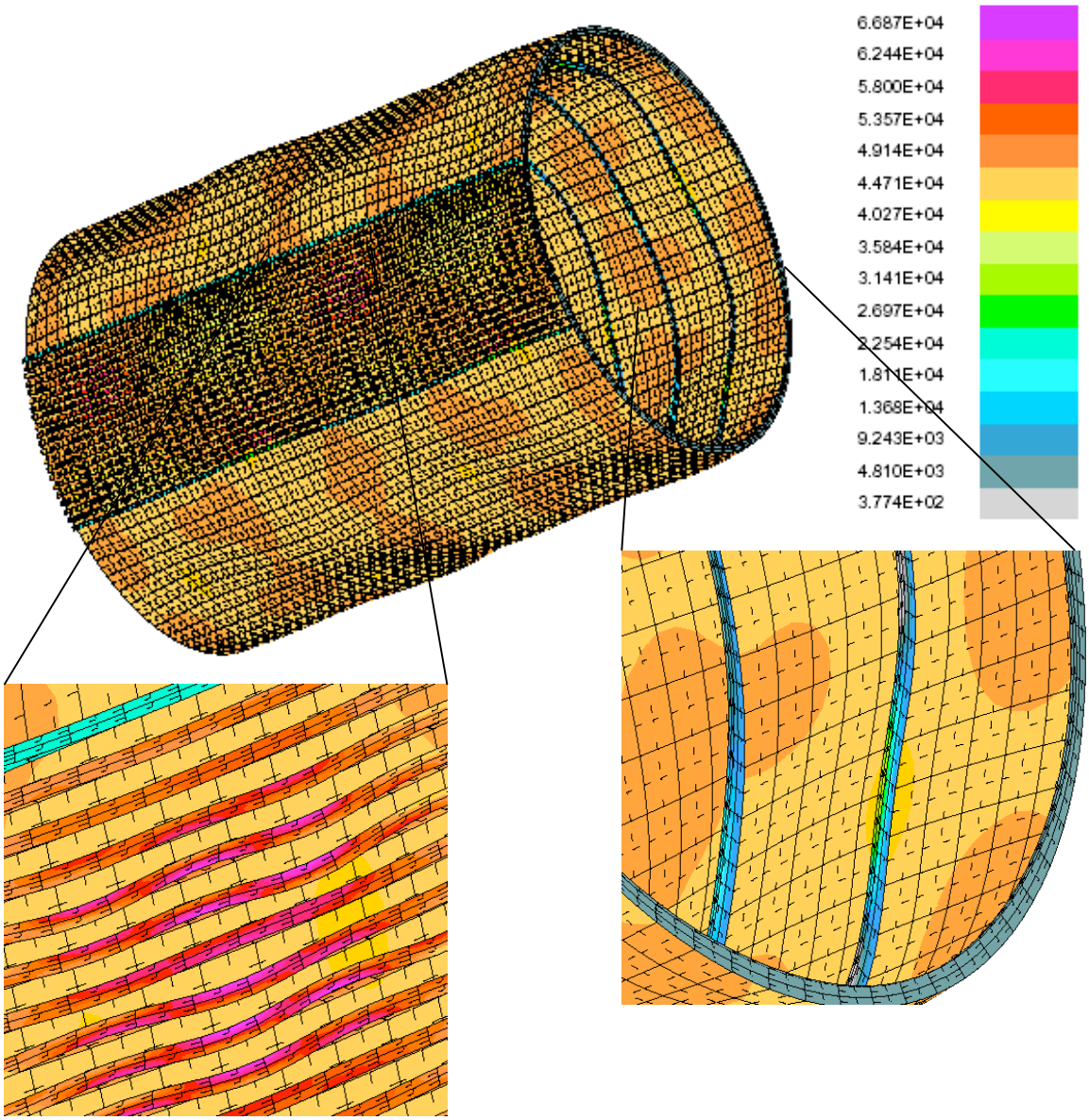

Case 4, Table 4: no Koiter, yes change imperfection, ICONSV=1; also see Figs. 61-63. Nonlinear equilibrium state from STAGS at the load factor, PA=1.00516. The imperfect shell has two initial buckling modal imperfection shapes: Fig. 1a with amplitude, Wimp1=+0.0625 and Fig. 61 with amplitude, Wimp2= -0.0005 inch. Prebuckling bending of the imperfect shell causes redistribution of stresses among the shell skin and the stiffener segments. Also, prebuckling bending gives rise to "flattened" regions with an "effective" circumferential radius of curvature that causes early general buckling. (See the right-most expanded insert).

FIG. 2 Outer fiber effective stress (psi) at axial load, Nx= -3000 x 1.00516 lb/in.

From: AIAA 48th Structures, Structural Dynamics, and Materials Conference, Paper no. AIAA-2007-2216, 2007

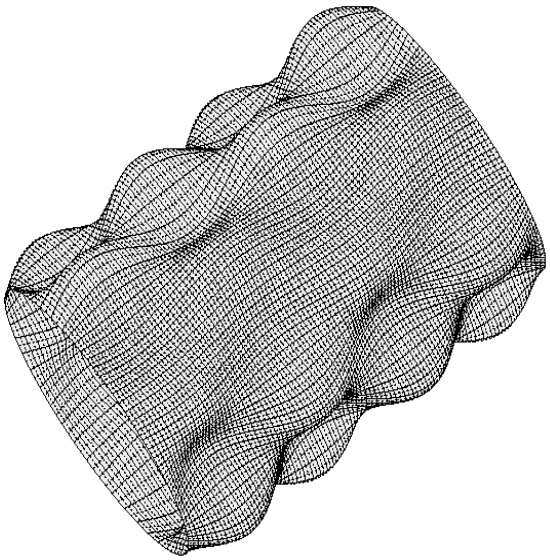

Case 2, Table 4 no Koiter, yes change imperfection, ICONSV= -1. Compare with Fig. 17. STAGS Mode no. 1, load factor, pcr=1.9189; PANDA2 predicts 1.890. The linear buckling mode agrees with that from PANDA2: (m,n)=(4,6) halfwaves over 180 deg. See Part 1, Run 1 of Table 9. **This is Fig. 16**

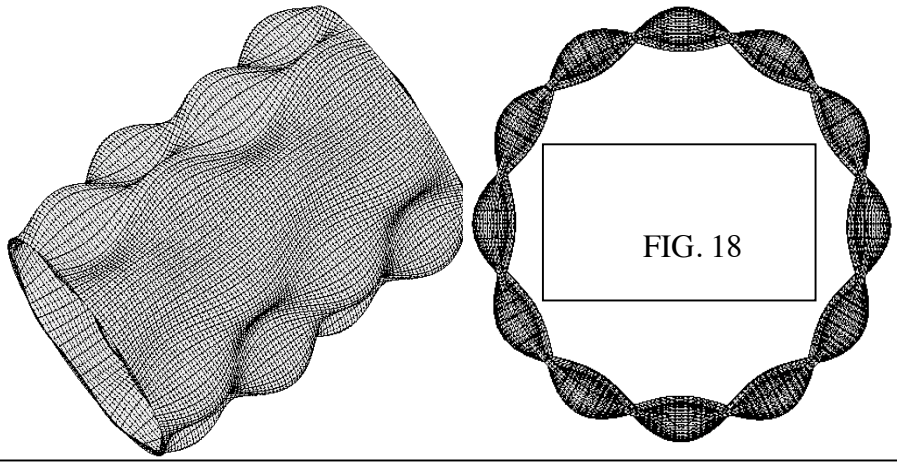

FIG. 18

Case 2, Table 4: no Koiter, yes change imperfection, ICONSV = -1; Compare with Fig. 16. STAGS Mode no. 1, load factor, pcr=1.9017; PANDA2 predicts 1.890. The linear buckling mode agrees with that from PANDA2: (m,n)=(4,6) halfwaves over 180 deg. See Part 1, Run 2 in Table 9. This STAGS model and the model in the previous figure are used to obtain good approximations of the general buckling mode shape and load factor (eigenvalue) for two reasons: 1. Determine what circumferential sector to use for more refined models (60 degrees is good in this case), and 2. obtain a good estimate of the initial eigenvalue "shift" to use in the more refined models. **These are Figs. 17 and**